Neurobiology of Stress 15 (2021) 100369

Contents lists available at ScienceDirect

Neurobiology of Stress

journal homepage: www.elsevier.com/locate/ynstr

Combinatorial actions of glucocorticoid and mineralocorticoid stress hormone receptors are required for preventing neurodegeneration of the mouse hippocampus

Robert H. Oakley [a], Shannon D. Whirledge [a], Maria G. Petrillo [a], Natallia V. Riddick [b], Xiaojiang Xu [c], Sheryl S. Moy [b], John A. Cidlowski [a,*]

[a] Signal Transduction Laboratory, National Institute of Environmental Health Sciences, National Institutes of Health, Research Triangle Park, NC, 27709, USA
[b] Department of Psychiatry and Carolina Institute for Developmental Disabilities, University of North Carolina at Chapel Hill, Chapel Hill, NC, 27599, USA
[c] Laboratory of Integrative Bioinformatics, National Institute of Environmental Health Sciences, National Institutes of Health, Research Triangle Park, NC, 27709, USA

ARTICLE INFO

Keywords:
Stress
Glucocorticoid
Glucocorticoid receptor
Mineralocorticoid receptor
Neurodegeneration
Neurogenesis

ABSTRACT

Chronic stress contributes to numerous human pathologies including cognition impairments and psychiatric disorders. Glucocorticoids are primary stress hormones that activate two closely related nuclear receptors, the glucocorticoid (GR) and mineralocorticoid receptor (MR), that are both highly expressed in the hippocampus. To investigate potential combinatorial actions of hippocampal GR and MR, we developed mice with conditional knockout of both GR and MR in the hippocampus and compared them to their single knockout counterparts. Mice lacking MR alone or both GR and MR in the hippocampus exhibited altered expression of multiple CA2-specific neuronal markers and enhanced cue-dependent learning in a conditioned fear test. Provocatively, in contrast to the single knockouts, mice depleted of both GR and MR showed profound neurodegeneration of the hippocampus. Neuronal death was increased and neurogenesis was reduced in the dentate gyrus of the double knockout mice. Global gene expression assays of the knockout mice revealed a synergistic increase in the number of dysregulated genes in the hippocampus lacking both GR and MR. This large cohort of genes reliant on both GR and MR for expression was strongly associated with cell death and cell proliferation pathways. GR/MR complexes were detected in CA1 and dentate gyrus neurons suggesting receptor heterodimers contribute to the joint actions of GR and MR. These findings reveal an obligate role for MR signaling in regulating the molecular phenotype of CA2 neurons and demonstrate that combinatorial actions of GR and MR are essential for preserving dentate gyrus neurons and maintaining hippocampal health.

1. Introduction

Stress contributes to numerous human pathologies including cognition impairment and psychiatric disorders (de Kloet et al., 2005). Glucocorticoids are primary stress hormones that are synthesized and released from the adrenal glands following activation of the hypothalamic-pituitary-adrenal (HPA) axis (Oakley and Cidlowski, 2013). These hormones are secreted in a diurnal pattern and acutely in response to physiological or emotional stress. Glucocorticoids act on nearly every cell and tissue of the body to maintain homeostasis, and their ability to suppress the immune system have made synthetic derivates of these hormones one of the most prescribed drug classes in the world today. The actions of glucocorticoids are mediated by the highly homologous glucocorticoid (NR3C1; here after GR) and mineralocorticoid receptors (NR3C2; here after MR) that are members of the nuclear receptor superfamily of ligand dependent transcription factors. MR binds endogenous glucocorticoids (cortisol in humans; corticosterone in rodents) with higher affinity than GR (Reul and de Kloet, 1985). Thus, MR is thought to be predominantly occupied by glucocorticoids under non-stressed conditions when HPA activity is low and to remain bound as HPA activity increases (De Kloet et al., 1998). GR, on the other hand, becomes progressively occupied by glucocorticoids as hormone levels rise during the circadian peak and in response to stress. Once bound by glucocorticoids, GR and MR regulate the expression of numerous genes by direct binding to nearly identical DNA sequences. Because of their molecular similarity, the specific and collaborative roles played by GR

* Corresponding author.
E-mail address: cidlows1@niehs.nih.gov (J.A. Cidlowski).

https://doi.org/10.1016/j.ynstr.2021.100369
Received 17 March 2021; Received in revised form 15 July 2021; Accepted 19 July 2021
Available online 21 July 2021

and MR in mediating the direct actions of stress on target tissues remain poorly understood.

In the brain, glucocorticoids act on the hippocampus to regulate learning, memory, and mood. A particularly striking feature of the hippocampus is that it expresses high levels of both GR and MR suggesting it is especially sensitive to stress (Seckl et al., 1991; Watzka et al., 2000). Indeed, sustained elevations in glucocorticoids resulting from chronic stress or prolonged glucocorticoid therapy lead to hippocampal alterations that have been associated with learning and memory deficits, depression, anxiety, and post-traumatic stress disorder (de Kloet et al., 2005). Pharmacological agents have been used to delineate hippocampal GR and MR activity; however, these studies are limited by ligand promiscuity and by their failure to discriminate between systemic and local signaling effects. Mice with conditional knockout of GR or MR in hippocampal neurons have also been developed to elucidate receptor function (Tronche et al., 1999; Gass et al., 2000; Boyle et al., 2005; Berger et al., 2006), but it is unclear whether observed phenotypes are due directly to the receptor that was depleted or indirectly to aberrant signaling properties of the remaining receptor. In addition, it remains unknown if GR and MR signaling pathways work together to regulate hippocampal function and whether loss of both receptors in the hippocampus leads to unique molecular and behavioral phenotypes. Understanding the signaling paradigms of GR and MR in the hippocampus is of utmost importance given the established role of chronic stress signaling to negatively influence intellectual and mental health.

We used a genetic approach to investigate potential combinatorial actions of hippocampal GR and MR by generating mice with conditional knockout of GR, MR, or both GR and MR in the hippocampus. Mice with knockout of MR alone or both GR and MR in the hippocampus showed a major loss of multiple CA2-specific neuronal markers and increased cue-dependent learning in a condition fear test. Provocatively, extensive neurodegeneration was observed only in the dentate gyrus of mice lacking both hippocampal GR and MR. Ablation of these two receptors in the double knockout hippocampus led to increased neuronal death and reduced neurogenesis. Global gene expression assays revealed major transcriptional reprogramming of the hippocampus in knockout mice. Compared to their single knockout counterparts, mice depleted of both GR and MR in the hippocampus exhibited a synergistic increase in the number of dysregulated genes. This large set of genes uniquely reliant on both GR and MR signaling for appropriate expression was strongly associated with cell death and cell proliferation pathways. Furthermore, GR/MR complexes were detected in the hippocampus and provide a unique mechanism for increasing the sensitivity and expanding the diversity of stress responses mediated by this dual receptor system. These findings reveal that MR signaling is necessary for the molecular phenotype of CA2 neurons and that combinatorial actions of GR and MR are required for preserving dentate gyrus neurons and maintaining hippocampal health.

2. Material and methods

2.1. Generation of $GR^{Emx1-cre}$, $MR^{Emx1-cre}$, and $GRMR^{Emx1-cre}$ mice

Mice with floxed GR locus ($GR^{fl/fl}$) (Oakley et al., 2013), floxed MR locus ($MR^{fl/fl}$) (McCurley et al., 2012), and with both alleles floxed ($GR^{fl/fl}MR^{fl/fl}$) have been described previously (Oakley et al., 2019). $GR^{fl/fl}$, $MR^{fl/fl}$, and $GR^{fl/fl}MR^{fl/fl}$ mice were each mated with mice expressing Cre recombinase under the direction of the empty spiracles homeobox 1 (*Emx1*) locus (The Jackson Laboratory, 005628). The resulting $GR^{fl/fl}Emx1^{Cre/+}$ ($GR^{Emx1-cre}$), $MR^{fl/fl}Emx1^{Cre/+}$ ($MR^{Emx1-cre}$), and $GR^{fl/fl}MR^{fl/fl}Emx1^{Cre/+}$ ($GRMR^{Emx1-cre}$) mice were on a C57BL/6NJ background. The $GR^{fl/fl}Emx1^{Cre/+}$ mice have been described previously (Tejos-Bravo et al., 2021). Cre negative $GR^{fl/fl}Emx1^{+/+}$ (GRflox), $MR^{fl/fl}Emx1^{+/+}$ (MRflox), and $GR^{fl/fl}MR^{fl/fl}Emx1^{+/+}$ (dflox) mice served as controls. Data presented are from male mice. Genotypes were determined using real time PCR with specific probes designed for each gene (Transnetyx). Mice were housed on a 12 h:12 h light/dark cycle with access to food and water *ad libitum*. All experiments on mice were approved and performed according to the guidelines of the Animal Care and Use Committee (NIEHS) and the Institutional Animal Care and Use Committee (UNC). All efforts were made to minimize animal suffering, to reduce the number of mice used, and to use alternatives to in vivo techniques, if available.

2.2. Real-time PCR

Total RNA from whole hippocampus was analyzed on a 7900HT (Applied Biosystems) or CFX96 (BioRad) sequence detection system. All primer sets for PCR were purchased from Applied Biosystems. Relative expression values for each gene were calculated using the double delta Ct analysis method and the housekeeping gene peptidylprolyl isomerase B (*Ppib*).

2.3. Immunoblotting

The hippocampus and cortex were removed from both hemispheres of each mouse and lysed in sodium dodecyl sulfate (SDS) sample buffer. Nitrocellulose membranes with equivalent amounts of protein were analyzed and quantitated using the Odyssey Infrared Imaging System (LI-COR Biosciences). Primary antibodies were to GR (Cell Signaling, #3660), MR (clone 6G1 generously provided by Dr. Celso E. Gomez-Sanchez) (Gomez-Sanchez et al., 2006), and actin (Millipore, #MAB1501). Goat anti-rabbit Alexa Fluor 680-conjugated (Life Technologies, #A21109) and goat anti-mouse IRDye800-conjugated (LI-COR Biosciences, #926–32210) secondary antibodies were utilized.

2.4. Corticosterone measurements

Mandibular bleeds were performed on adult male mice on three occasions separated by at least one week: in the morning (between 8:30 and 9:30 a.m.), evening (between 7:00 and 8:30 p.m.), and immediately following restraint stress. For restraint stress, mice were placed in ventilated holders (Kent Scientific) for 30 min, and these experiments were carried out in the morning (between 7:00 and 9:30 a.m.). Serum corticosterone levels were measured using an Enzyme Immunoassay Kit (Arbor Assays, Ann Arbor, MI).

2.5. Histological analysis

Control and knockout mice were perfused transcardially with saline followed by 4 % paraformaldehyde. Brains were removed, fixed in 4 % paraformaldehyde for 24 h, cryoprotected in 30 % sucrose in PBS for 48 h, and then frozen in embedding medium (OCT, Sakura Finetek, Torrance, CA). Coronal sections (40 μm) were collected using a cryostat. Free floating sections were stored at 4 °C in phosphate buffered saline (PBS) supplemented with sodium azide (0.01 %). For some experiments, brains were embedded in paraffin and 8-μm coronal sections were collected using a vibratome and mounted on slides. Nissl stains were performed on 40-μm sections according to standard protocols. The thickness of the dorsal blade of the dentate gyrus was determined from Nissl-stained sections using NIH Image J (FIJI) software. Three measurements were taken (beginning, middle, end) along an approximate 350 μm section of the dentate gyrus that was similarly located in both the dflox and $GRMR^{Emx1-cre}$ mice. For immunofluorescence studies, 40-μm free floating sections were processed for antigen retrieval by boiling in a citrate-based antigen unmasking solution (Vector Laboratories) for 5 min. Primary antibodies were rabbit anti-GR (Cell Signaling, #3660), mouse anti-MR (clone 6G1) (Gomez-Sanchez et al., 2006), rabbit anti-PCP4 (Sigma-Aldrich, #HPA005792), mouse anti-RGS14 (Antibodies Incorporated, #75–170), and mouse anti-PCP4 (Sigma-Aldrich, #AMAB91359). Secondary antibodies were goat anti-mouse Alexa Fluor 488 (Life Technologies, #A11001) and goat anti-rabbit Alexa Fluor 594

(Life Technologies, #A11012). Slides were mounted using VECTASHIELD antifade mounting medium with DAPI (Vector Laboratories). For Ki67 and doublecortin (DCX) staining, paraffin sections were deparaffinized, rehydrated, and processed as above for immunofluorescence using rabbit anti-Ki67 (Cell Signaling, #12202) or rabbit anti-DCX (Cell Signaling, #4604) primary antibodies. Mouse anti-NeuN Alexa Fluor 488-conjugated primary antibody (EMD Millipore, MAB377X) was also used in conjunction with DCX staining. Ki67-positive cells and DCX-positive cells were counted in the dentate gyrus from 2 different sections from each hemisphere of 3 different mice per genotype (total of 12 sections). The TUNEL assay was performed on paraffin sections using the ApopTag Fluorescein In Situ Apoptosis Detection Kit (Millipore). TUNEL-positive nuclei were counted in the dentate gyrus from 2 different sections from each hemisphere of 3 different mice per genotype (total of 12 sections). Images were captured using an epifluorescence or laser confocal microscope (Zeiss LSM 780). Hematoxylin and eosin staining was performed on paraffin sections according to standard protocols.

2.6. Microarray analysis

Global gene expression analysis was performed on RNA isolated from the whole hippocampus from ~2.5-month old dflox, $GR^{Emx1-cre}$, $MR^{Emx1-cre}$, and $GRMR^{Emx1-cre}$ mice (n = 3–4 mice per genotype). The Agilent Whole Mouse Genome oligo arrays (014868) (Agilent Technologies) was used following the Agilent 1-color microarray-based gene expression analysis protocol as described previously (Oakley et al., 2019). To determine differentially expressed probes, an ANOVA with multiple test correction (FDR q-value < 0.05) was performed using Partek Genomics Suite software, version 6.6 (Partek). Heat maps of differentially expressed genes were generated using hierarchical clustering. The statistically significant probes were analyzed by Ingenuity Pathway Analysis (IPA) software (Ingenuity Systems). Gene enrichment P values (p-value < 0.05) were determined by IPA using Fisher's exact test. Microarray data have been deposited in Gene Expression Omnibus with the accession number "GSE149625."

2.7. Behavioral assays

Behavioral assays were performed during the light phase of the light/dark cycle. Control mice were comprised of 8–10 GRflox, 7–8 MRflox, and 10 dflox mice. Separate analysis of these 3 wild-type groups revealed no significant differences in any of the tests. Knockout mice were comprised of 12 $GR^{Emx1-cre}$, 11–12 $MR^{Emx1-cre}$, and 9–12 $GRMR^{Emx1-cre}$ mice.

2.8. Conditioned fear test

Mice ~12 weeks old were evaluated for learning and memory in a conditioned fear test (Near-Infrared image tracking system, MED Associates, Burlington, VT). The procedure had the following phases: training on Day 1, a test for context-dependent learning on Day 2, and a test for cue-dependent learning on Day 3. Two weeks following the first tests, mice were given second tests for retention of contextual and cue learning. For training on Day 1, each mouse was placed in the test chamber, allowed to explore for 2 min, and then exposed to a 30-sec tone (80 dB) that co-terminated with a 2-sec scrambled foot shock (0.4 mA). Mice received 2 additional shock-tone pairings, with 80 s between each pairing. On Day 2 and 16, mice were placed back into the original conditioning chamber for a test of contextual learning. Levels of freezing were determined across a 5-min session. On Day 3 and 17, mice were placed in a modified conditioning chamber for a test of cue learning. The conditioning chambers were modified using a Plexiglas insert to change the wall and floor surface, and a novel odor (dilute vanilla flavoring) was added to the sound-attenuating box. Mice were placed in the modified chamber and allowed to explore. After 2 min, the acoustic stimulus (an 80 dB tone) was presented for a 3-min period. Levels of freezing before and during the stimulus were determined across a 5-min session.

2.9. Accelerating rotarod test

Mice ~10 weeks old were tested for motor coordination and learning on an accelerating rotarod (Ugo Basile, Stoelting Co., Wood Dale, IL). For the first test session, mice were given three trials, with 45 s between each trial. Two additional trials were given 48 h later. Rpm (revolutions per minute) was set at an initial value of 3, with a progressive increase to a maximum of 30 rpm across 5 min (the maximum trial length). Measures were taken for latency to fall from the top of the rotating barrel.

2.10. Acoustic startle test

Mice ~11 weeks old and ~16 weeks old were tested for auditory function, reactivity to environmental stimuli, and sensorimotor gating using the acoustic startle test. Mice were placed into individual small Plexiglas cylinders within larger, sound-attenuating chambers. Each cylinder was seated upon a piezoelectric transducer, which allowed vibrations to be quantified and displayed on a computer (San Diego Instruments SR-Lab system). The chambers included a ceiling light, fan, and a loudspeaker for the acoustic stimuli. Background sound levels (70 dB) and calibration of the acoustic stimuli were confirmed with a digital sound level meter (San Diego Instruments). Each session consisted of 42 trials, that began with a 5-min habituation period. There were 7 different types of trials: the no-stimulus trials, trials with the acoustic startle stimulus (40 msec; 120 dB) alone, and trials in which a prepulse stimulus (20 msec; either 74, 78, 82, 86, or 90 dB) occurred 100 ms before the onset of the startle stimulus. Measures were taken of the startle amplitude for each trial across a 65-msec sampling window, and an overall analysis was performed for each subject's data for levels of prepulse inhibition at each prepulse sound level [calculated as 100 - (response amplitude for prepulse stimulus and startle stimulus together/response amplitude for startle stimulus alone x 100].

2.11. Proximity ligation assay (PLA)

PLA was performed using the Duolink™ In Situ Red Kit Mouse/Rabbit (Millipore Sigma). Brains were embedded in paraffin and 8-μm coronal sections were collected using a vibratome and mounted on slides. After deparaffinization, rehydration, and antigen retrieval steps, sections were permeabilized with PBS containing 2 % BSA and 0.1 % Tween-20 for 30 min at room temperature, and incubated with the Duolink blocking solution for 1 h at 37 °C. The sections were then incubated with the rabbit anti-GR antibody (Cell Signaling, #3660) and mouse anti-MR antibody (clone 6G1) (Gomez-Sanchez et al., 2006), followed by incubation with the secondary PLA probes, anti-rabbit PLA-minus and anti-mouse PLA-plus. After washing, ligase and amplification steps were performed according to the manufacturer's protocol, with the exception that the amplification step was prolonged to 2 h. Samples were then washed, air-dried, and mounted with Vectashield antifade mounting medium with DAPI. For each hippocampus, a negative control was performed omitting the anti-MR antibody. To quantify the PLA signals (puncta), z-stack images were acquired using a Zeiss laser-scanning confocal microscope (LSM 880, Carl Zeiss) and analyzed using Imaris 9.5 software (Oxford Instruments). The same fluorescence threshold and size threshold of PLA puncta was applied equally to all images. For each hippocampal region investigated, the number of puncta measured was divided by the area investigated (puncta per μm^2) and the value of the negative control was subtracted.

2.12. Statistics

An unpaired two-tailed *t*-test, one-way ANOVA with Tukey's multiple comparisons test, or two-way repeated measures ANOVA with

Tukey's multiple comparisons test were used to evaluate statistical significance (defined as p-value < 0.05). The Mantel-Cox log-rank test was used for survival curves. The statistical analyses were performed using GraphPad Prism software (version 7.02). Data distribution was assumed to be normal, but this was not formally tested.

3. Results

3.1. Development of $GR^{Emx1-cre}$, $MR^{Emx1-cre}$, and $GRMR^{Emx1-cre}$ mice

To delineate the individual and combinatorial actions of GR and MR in mediating the direct effects of glucocorticoids in the hippocampus, we developed mice on a C57BL/6 background with conditional knockout of GR ($GR^{Emx1-cre}$), MR ($MR^{Emx1-cre}$), or both GR and MR ($GRMR^{Emx1-cre}$) in the hippocampus using empty spiracles homeobox 1 (*Emx1*) promoter-driven Cre recombinase mice (Gorski et al., 2002). We evaluated the expression of GR and MR in flox control and knockout mice using RNA and protein lysates prepared from the whole hippocampus (Fig. 1A–B). The $GR^{Emx1-cre}$ mice showed decreased levels of GR mRNA and protein in the hippocampus and no change in MR. The $MR^{Emx1-cre}$ mice showed reduced levels of MR in the hippocampus and, interestingly, an upregulation in GR. GR mRNA was increased 1.69-fold and a similar 1.45-fold increase in GR protein was measured. Both GR and MR were reduced in the hippocampus from $GRMR^{Emx1-cre}$ mice. The upregulation of GR in the $MR^{Emx1-cre}$ hippocampus suggests that MR normally functions to suppress GR expression in this brain region and reveals a new mode of crosstalk between these two receptors. The increase in GR further suggests that aberrant GR signaling, rather than the loss of MR signaling, may contribute to any phenotypes that develop in the $MR^{Emx1-cre}$ mice and highlights the importance of having mice lacking both receptors in the hippocampus for distinguishing between these two scenarios.

In addition to the hippocampus, *Emx1*-cre mediated recombination has been reported to occur in other regions of the forebrain (Gorski et al., 2002; Xie et al., 2019). To assess the pattern of Cre recombination in the forebrain of our knockout mice, we evaluated GR levels by immunofluorescence staining in the GRflox and $GR^{Emx1-cre}$ mice. GR was chosen as a sensitive readout for this analysis because it is ubiquitously expressed in the brain whereas MR exhibits a more restricted distribution (Reul and de Kloet, 1985). Consistent with the hippocampal RTPCR and immunoblot data (Fig. 1A–B), GR expression was markedly reduced in the hippocampus of the $GR^{Emx1-cre}$ mice (Supplemental Figure 1). In these same brain sections, we also detected a loss of GR expression in the cortex, basomedial amygdala, and basolateral amygdala. GR levels were not altered in the central amygdala, thalamus, and hypothalamus. This recombination pattern is in agreement with previous reports assessing Cre activity in the forebrain of the *Emx1*-cre mice (Gorski et al., 2002; Xie et al., 2019). We further characterized the Cre recombination occurring in the cortex by quantifying GR and MR protein levels in each of our knockout mouse models. Immunoblot analysis of cortex lysates showed reduced expression of GR and no change in MR levels in the $GR^{Emx1-cre}$ mice, reduced expression of MR and no change in GR levels in the $MR^{Emx1-cre}$ mice, and decreased expression of both GR and MR in the $GRMR^{Emx1-cre}$ mice (Supplemental Figure 2). Interestingly, in contrast to our findings in the hippocampus, the loss of MR in the cortex did not lead to an upregulation of GR suggesting the ability of MR to limit GR expression occurs in a brain region-specific manner. These data demonstrate that *Emx1*-cre mediated deletion of GR and/or MR is not restricted to the hippocampus but also occurs in several other forebrain regions of the knockout mice.

The $GR^{Emx1-cre}$, $MR^{Emx1-cre}$, and $GRMR^{Emx1-cre}$ mice were born at the expected Mendelian ratio and survived normally through 12 months of age (Fig. 1C). The $GR^{Emx1-cre}$ mice showed normal growth with no alteration in body weight throughout the 12-month study (Fig. 1D). In contrast, significant reductions in body weight were observed at 3 and 6 months for the $MR^{Emx1-cre}$ mice (14.4 % and 12.2 % decrease compared to MRflox control mice, respectively) and at 6 and 12 months for the $GRMR^{Emx1-cre}$ mice (13.0 % and 15.5 % decrease compared to dflox control mice, respectively). Morning (circadian nadir) and evening (circadian peak) corticosterone levels did not differ among the single and double knockout mice (Fig. 1E). In addition, no genotype differences were observed for peak corticosterone levels following 30 min of restraint stress (Fig. 1E). These findings suggest that both circadian and stress induced activation of the HPA axis remain intact in the $GR^{Emx1-cre}$, $MR^{Emx1-cre}$, and $GRMR^{Emx1-cre}$ mice. To evaluate whether the loss of GR, MR, or both receptors affected the morphology of the hippocampus, we performed Nissl staining on brain slices from 3-month old flox control and knockout mice (Fig. 1F). The $GR^{Emx1-cre}$, $MR^{Emx1-cre}$, and $GRMR^{Emx1-cre}$ hippocampi showed no gross abnormalities in the density of pyramidal neurons in the CA1, CA2, and CA3 subfields and granule neurons of the dentate gyrus suggesting GR and MR signaling are not required for hippocampal formation in mice.

3.2. Hippocampal MR signaling is required to maintain the molecular phenotype of CA2 neurons

We evaluated the distribution of GR and MR in the hippocampus of the knockout mice in order to determine if depletion of one receptor altered the distribution pattern of the remaining receptor. In flox control mice, GR protein was detected in the CA1, CA2, CA3, and dentate gyrus; however, the level of expression differed across these regions (Fig. 2A). GR was abundant in the CA1 and dentate gyrus but exhibited lower expression in the CA2 and CA3. Higher magnification images depict the marked difference in GR expression between the CA1 and CA2/CA3 subfields (Fig. 2B). Using the CA2-specific marker regulator of G protein signaling 14 (RGS14) (Evans et al., 2015), we confirmed that the change in GR expression occurred at the CA1/CA2 boundary (Fig. 3A). MR expression was also detected in the CA1, CA2, CA3, and dentate gyrus (Fig. 2A). In contrast to GR, MR was more abundant in the CA2 and CA3 than in the CA1 and the dentate gyrus. Higher magnification images show the increased expression of MR in the CA2/CA3 regions compared to CA1 (Fig. 2B). Using the CA2-specific marker Purkinje cell protein 4 (PCP4) (Evans et al., 2015), we confirmed that the change in MR expression occurred at the CA1/CA2 boundary (Fig. 3A). In all regions of the hippocampus, both GR and MR were found to colocalize in the same neurons (Fig. 2B and Supplemental Figures 3–5). These distinct patterns of hippocampal GR and MR expression indicate that the relative level of these 2 nuclear receptors differs dramatically between the CA1 and dentate gyrus neurons and the CA2 and CA3 neurons.

In the $GR^{Emx1-cre}$ mice, GR expression was abolished in all regions of the hippocampus and MR expression was unaffected (Fig. 2 and Supplemental Figures 3–5). MR expression was abolished throughout the hippocampus of the $MR^{Emx1-cre}$ mice (Fig. 2 and Supplemental Figures 3–5). However, in these same mice, GR expression was elevated in the hippocampus, particularly in the CA2 and CA3 subfields that normally express low levels of GR (Fig. 2 and Supplemental Figure 4). The upregulated expression of GR in the CA2 and CA3 has been observed in other mouse models with knockout of hippocampal MR and accounts for the increase in GR expression that we observed in the hippocampal lysates prepared from the $MR^{Emx1-cre}$ mice (Fig. 1A–B) (Berger et al., 1998;ter Horst et al., 2012). Consistent with our immunoblot data on the cortex (Supplemental Figure 2), the increase in GR expression following MR depletion appears to be specific to the CA2/CA3 regions of the hippocampus as no alteration in GR staining was observed in the cortex, basomedial amygdala, or basolateral amygdala of the $MR^{Emx1-cre}$ mice (Supplemental Figure 6). For the $GRMR^{Emx1-cre}$ mice, both GR and MR expression were abolished in all regions of the hippocampus (Fig. 2 and Supplemental Figures 3–5).

CA2 pyramidal neurons can be distinguished from CA1 neurons in flox control mice by their reduced expression of GR (Figs. 2B and 3A). This demarcation is lost, however, with the upregulation of GR in the $MR^{Emx1-cre}$ mice (Fig. 2B). Thus, to identify the CA2 neurons in the

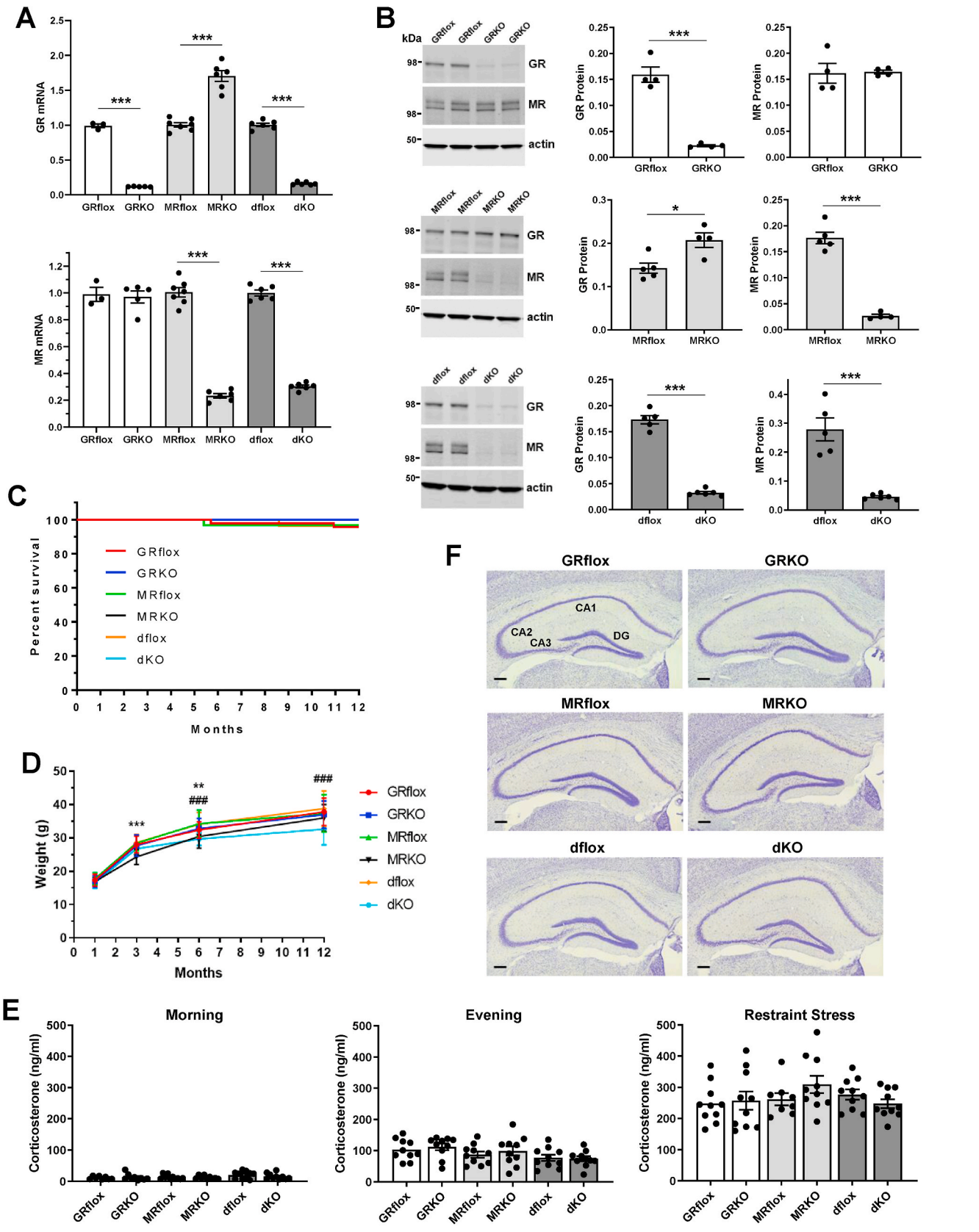

(caption on next page)

Fig. 1. Mice with conditional knockout of GR, MR, or both GR and MR in the hippocampus. (**A**) RTPCR of GR and MR mRNA from the hippocampus of ~3-month old male $GR^{Emx1-cre}$ (GRKO), $MR^{Emx1-cre}$ (MRKO), and $GRMR^{Emx1-cre}$ (dKO) mice. Data are mean ± SEM (n = 3–7 mice per group). A one-way ANOVA followed by Tukey post-hoc analysis was performed to determine significance. (**B**) Representative immunoblots and quantitation of GR and MR protein levels from the hippocampus of 2- to 5-month old male mice. Data are mean ± SEM (n = 4–6 mice per group). Student's *t*-test was performed to determine significance. (**C**) Survival curves for male GRflox (n = 46), $GR^{Emx1-cre}$ (n = 26), MRflox (n = 30), $MR^{Emx1-cre}$ (n = 31), dflox (n = 27), and $GRMR^{Emx1-cre}$ (n = 22) mice. Mantel-Cox log-rank test revealed no significant differences among genotypes. (**D**) Body weights were measured for male flox control and knockout mice at 1, 3, 6, and 12 months of age. Data are mean ± SEM (n = 11–39 mice per group). A one-way ANOVA followed by Tukey post-hoc analysis was performed to determine significance. (**E**) Corticosterone levels in the morning, evening, and immediately following 30 min of restraint stress in adult male mice. Data are mean ± SEM (n = 8–10 mice per group). A one-way ANOVA revealed no significance differences among genotypes. (**F**) Representative Nissl stains of brain sections from ~3-month old male mice (n = 3–4 mice per genotype). Scale bars, 200 μm. *P < 0.05 and **P < 0.01 for MRKO compared to MRflox. ***P < 0.001 for GRKO compared to GRflox, for MRKO compared to MRflox, and for dKO compared to dflox. ###P < 0.001 for dKO compared to dflox.

$MR^{Emx1-cre}$ mice, we performed immunofluorescence with antibodies for the CA2-specific markers, PCP4 and RGS14 (Fig. 3B). Both markers showed pronounced staining of CA2 neurons in flox control mice. However, for the $MR^{Emx1-cre}$ mice, there was a dramatic loss of PCP4 and RGS14 staining in the area where CA2 neurons are found. The density and size of the neurons in this anatomical region are consistent with CA2 morphology; however, the absence of PCP4 and RGS14 staining suggests the molecular profile of these neurons has been altered. In contrast to the $MR^{Emx1-cre}$ mice, the $GR^{Emx1-cre}$ hippocampus showed normal PCP4 and RGS14 staining of CA2 neurons (Fig. 3B). The molecular culprit responsible for the change in PCP4 and RGS14 expression in the $MR^{Emx1-cre}$ CA2 neurons could be either the loss of MR signaling or aberrant GR signaling. The latter may be particularly relevant in these mice given the pronounced upregulation of GR that occurs in CA2 neurons (Fig. 2). Mice lacking both GR and MR in the hippocampus distinguish between these two possibilities since GR expression is eliminated. As shown in Fig. 3B, the $GRMR^{Emx1-cre}$ mice phenocopy the $MR^{Emx1-cre}$ mice and exhibit a dramatic loss of PCP4 and RGS14 staining of the CA2 neurons, indicating that it is the deficiency of MR signaling rather than aberrant GR signaling that is responsible for this change. These data reveal a novel role for MR signaling in maintaining the molecular phenotype of CA2 neurons.

3.3. Global transcriptional profiles in the hippocampus of the $GR^{Emx1-cre}$, $MR^{Emx1-cre}$, and $GRMR^{Emx1-cre}$ mice

To identify the genes that are altered in the hippocampus of the single and double knockout mice, we performed a genome-wide microarray on hippocampal RNA from ~2.5-month old mice. A heat map of the samples and hierarchical clustering analysis revealed major transcriptional reprogramming of the knockout hippocampi (Fig. 4A). Knockout of hippocampal GR, MR, or both GR and MR resulted in the dysregulation of 413, 1478, and 3637 genes, respectively (Fig. 4B). The synergistic increase in the number of genes dysregulated in the $GRMR^{Emx1-cre}$ hippocampus was unanticipated and suggests not only that many genes rely on both GR and MR for their appropriate expression but that combinatorial actions of these two receptors comprise a chief component of the hippocampal stress response. Comparison of the 3 gene sets shows that 2438 genes were uniquely altered only when both GR and MR are depleted in the hippocampus (Fig. 4C). The microarray also revealed that a greater number of genes were altered in the $MR^{Emx1-cre}$ hippocampus compared to the $GR^{Emx1-cre}$ hippocampus (Fig. 4B). This result likely reflects our experiment being performed in mice under basal conditions when MR occupancy by glucocorticoids is favored. The gene set comparison shows that the majority of genes dysregulated in the $MR^{Emx1-cre}$ hippocampus (1034 of 1478, or 70.0 %) were also commonly dysregulated in the $GRMR^{Emx1-cre}$ hippocampus, indicating these gene changes were due to the loss of MR signaling rather than aberrant GR signaling. This pronounced overlap may account for the similar alterations in body weight and CA2 molecular profile observed for these two mouse models. Representative members of the genes uniquely altered only in the $GRMR^{Emx1-cre}$ hippocampus or commonly altered in both the $MR^{Emx1-cre}$ and $GRMR^{Emx1-cre}$ hippocampi were validated using RNA isolated from an independent set of mice (Fig. 4D–E).

Ingenuity pathway analysis (IPA) was utilized to investigate the diseases and biological functions most significantly associated with the dysregulated genes in each mouse model (Fig. 5A). Organismal Injury and Abnormalities was the highest ranked annotation associated with the genes altered in the $GR^{Emx1-cre}$ hippocampus. Behavior was the top-ranked annotation associated with the dysregulated genes in the hippocampus of the $MR^{Emx1-cre}$ mice and the 4th ranked annotation for the $GRMR^{Emx1-cre}$ mice consistent with the known role of glucocorticoids to influence behavioral adaptation to stress (de Kloet et al., 2005). Within the Behavior category, Cognition was the highest ranked specific behavior associated with the dysregulated genes in both the $MR^{Emx1-cre}$ and $GRMR^{Emx1-cre}$ hippocampi (Fig. 5B). Nervous System Development and Function was the top-ranked annotation for the dysregulated genes in the $GRMR^{Emx1-cre}$ hippocampus and the 5th ranked annotation for the $MR^{Emx1-cre}$ mice (Fig. 5A). The strong association with nervous system development in these two mouse models is consistent not only with the known role of glucocorticoids to influence neuronal differentiation but also with their shared molecular reprogramming of CA2 neurons (Fig. 3B). The similar gene enrichment results for the mice lacking MR alone or both GR and MR in the hippocampus reflects the large number of genes commonly dysregulated in these two mouse models.

We also used IPA to examine the cellular signaling pathways that were most significantly associated with the dysregulated genes in each knockout hippocampus (Fig. 5C). Interestingly, most of the top signaling pathways involve GPCRs. GPCRs are critical for apelin signaling and Wnt/GSK3beta signaling that are both strongly associated with the dysregulated genes in $GR^{Emx1-cre}$ hippocampus. In addition, GPCRs mediate CCR5 signaling and GNRH signaling that are among the top pathways associated with the dysregulated genes in the $MR^{Emx1-cre}$ and $GRMR^{Emx1-cre}$ hippocampi, respectively. Gene changes occurring in both the $MR^{Emx1-cre}$ and $GRMR^{Emx1-cre}$ hippocampi were also strongly associated with opioid signaling that is mediated by GPCRs and with G beta gamma signaling which serves as a primary intracellular transducer for activated GPCRs. In fact, G beta gamma signaling was predicted to have significantly increased activity (z-score > 2) in the mice lacking both GR and MR. These gene enrichment results suggest that GR and MR may preferentially target components of GPCR signaling pathways for mediating many of the direct effects of stress on the hippocampus.

3.4. Hippocampal GR and MR have distinct roles in learning and memory

The genes dysregulated in both the $MR^{Emx1-cre}$ and $GRMR^{Emx1-cre}$ hippocampi were strongly associated with cognition (Fig. 5B). Therefore, we evaluated the single and double knockout mice for alterations in learning and memory using a conditioned fear test. For training on Day 1, mice were placed in the conditioning chamber, allowed to explore for 2 min, and then exposed to 3 shock-tone pairings. To investigate contextual learning, mice were placed back in the original conditioning chamber on Day 2 and Day 16 and levels of freezing were determined across a 5-min session (Fig. 6A). The $GR^{Emx1-cre}$ mice exhibited reduced levels of freezing in the first test that was dependent on the time in the session. During the second test for memory retention on Day 16, significant effects of genotype were also observed; however, post-hoc

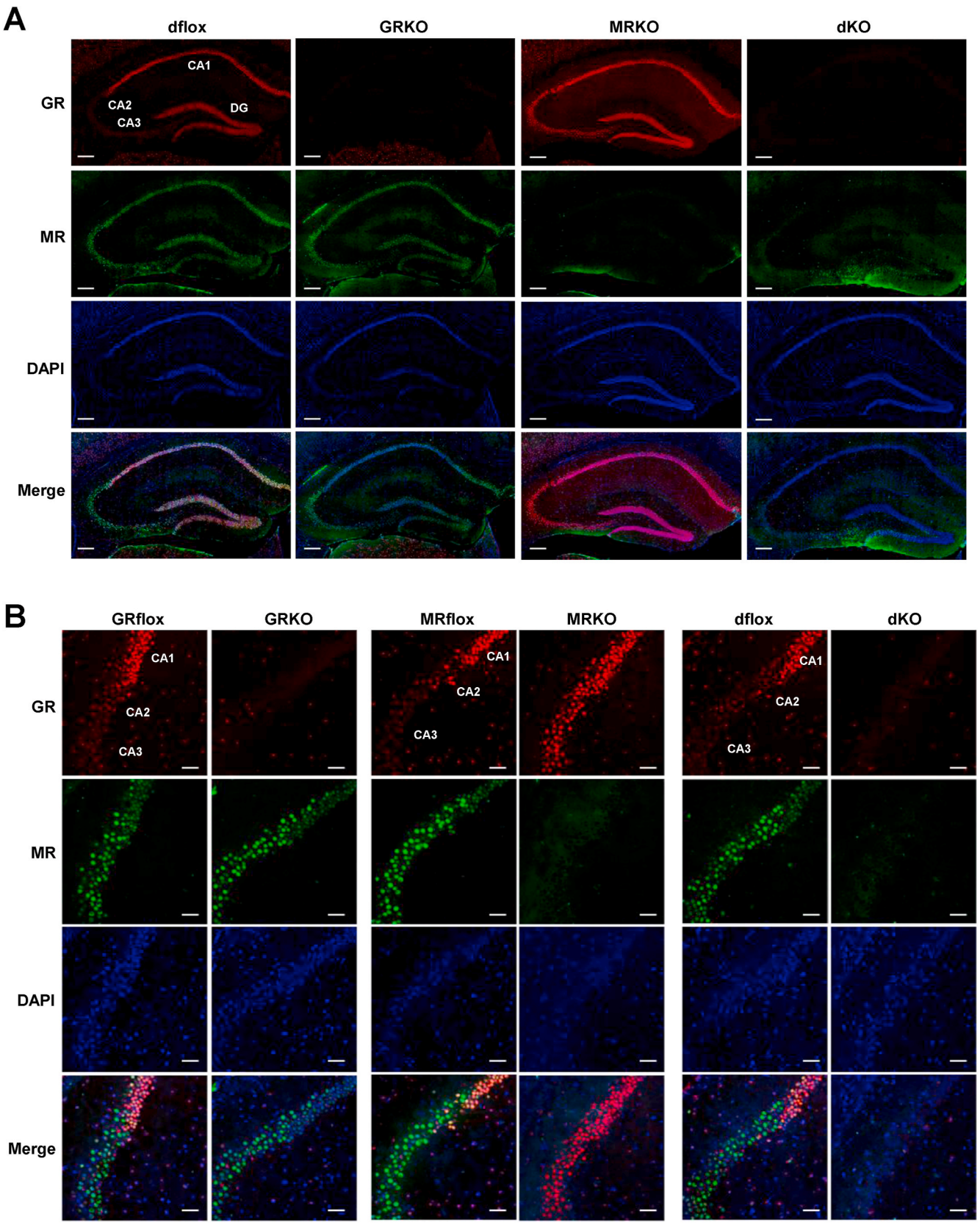

Fig. 2. Distribution of GR and MR in the hippocampus of control and knockout mice. Immunofluorescence analysis of GR and MR expression was performed on hippocampal sections from ~3.5-month old male flox control and knockout mice. (**A**) Representative images of the distribution of GR and MR in the whole hippocampus (n = 3 mice per genotype). Scale bars, 200 μm. (**B**) Representative images of the distribution of GR and MR at the CA1/CA2 boundary (n = 3 mice per genotype). Scale bars, 50 μm.

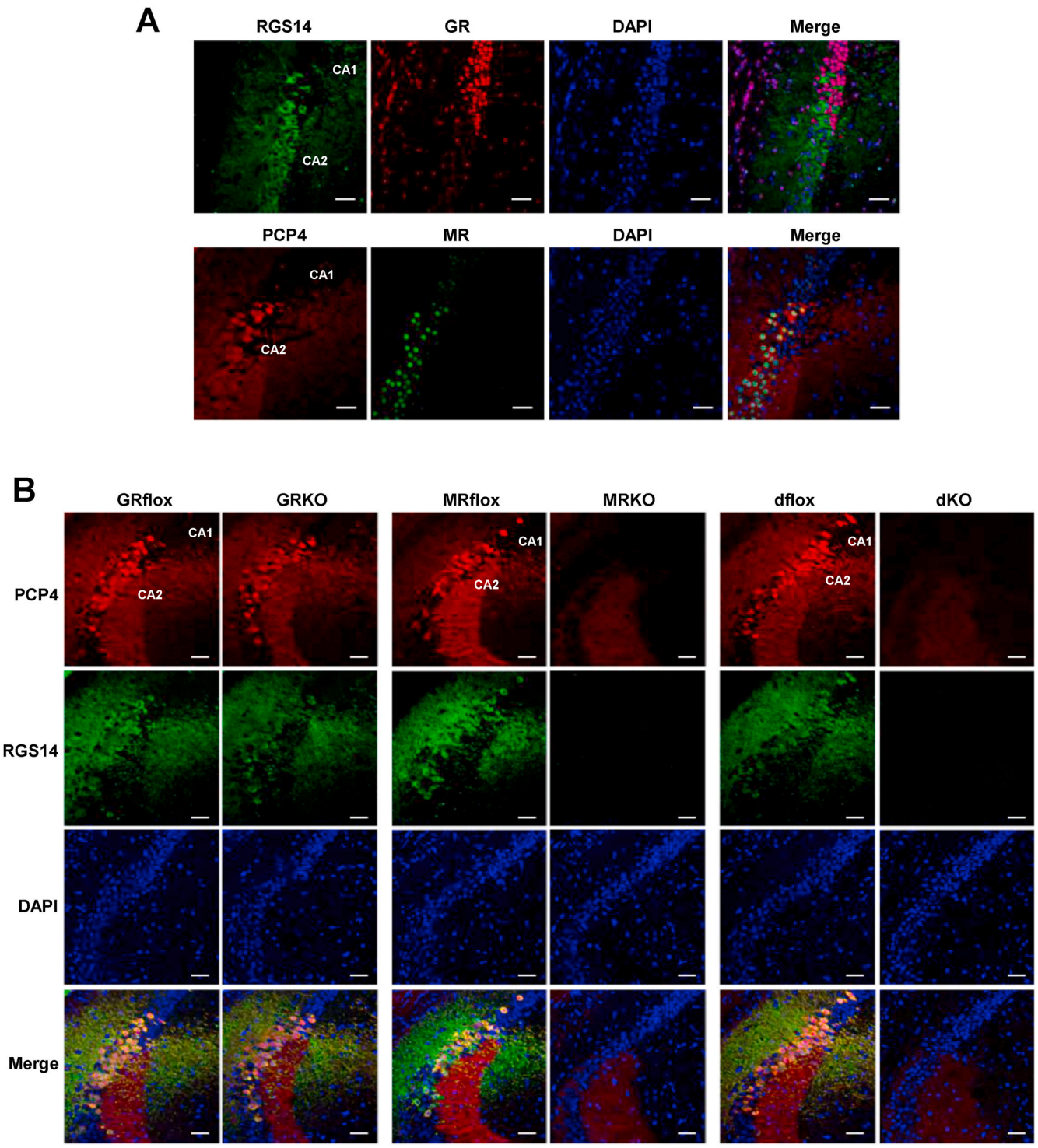

Fig. 3. Expression of CA2-specific neuronal markers is abolished in the hippocampus of MR$^{Emx1\text{-cre}}$ and GRMR$^{Emx1\text{-cre}}$ mice. Immunofluorescence was performed on hippocampal sections from ~3.5-month old male flox control and knockout mice. (**A**) Representative images of the distribution of RGS14 and GR (upper panels) and PCP4 and MR (lower panels) at the CA1/CA2 boundary in flox control mice (n = 3 mice per genotype). (**B**) Representative images of the distribution of the CA2-specific neuronal markers PCP4 and RGS14 in the CA1 and CA2 regions of the hippocampus from flox control and knockout mice (n = 3 mice per genotype). Scale bars, 50 μm.

analyses did not reveal significant group differences at any one time point. To evaluate cue-dependent learning, mice were placed in a modified conditioning chamber on Day 3 and Day 17 (Fig. 6B). Levels of freezing were determined before and during the acoustic stimulus for the 5-min session. The MR$^{Emx1-\text{cre}}$ mice exhibited higher levels of freezing during the first test, as well as two weeks later during the second test for memory retention. During the second test, the GRMR$^{Emx1-\text{cre}}$ mice also exhibited increased freezing at the 5-min time point and a trend (p-value = 0.08) towards an increase at the 4-min time point. Importantly, the observed alterations in the conditioned fear test could not be attributed to motor or hearing deficits (Supplemental Figures 7–8). The similar phenotype of the MR$^{Emx1-\text{cre}}$ and

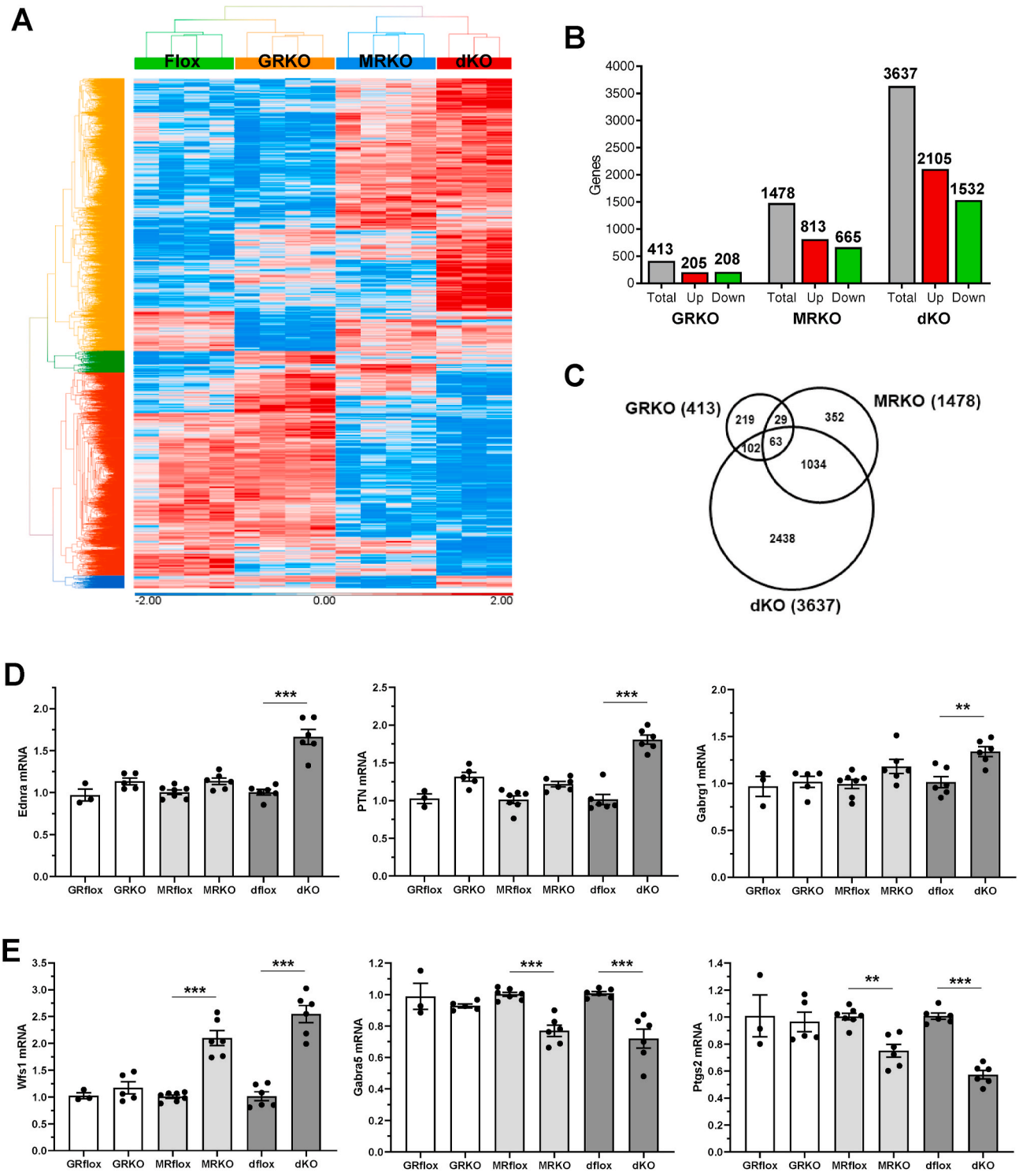

Fig. 4. Global gene expression profiles in the hippocampus of GR$^{Emx1\text{-cre}}$, MR$^{Emx1\text{-cre}}$, and GRMR$^{Emx1\text{-cre}}$ mice. A genome-wide microarray was performed on RNA isolated from the hippocampus of ~2.5-month old male flox control and knockout mice. (**A**) Heat map with hierarchical clustering of genes that were differentially expressed between flox control and knockout mice. (**B**) Total number of genes differentially expressed in the hippocampus of knockout mice compared to flox control mice. (**C**) Differentially expressed genes in the hippocampus of the knockout mice were compared using a Venn diagram. (**D**) RTPCR of endothelin receptor type A (*Ednra*), pleiotrophin (*PTN*), and gamma-aminobutyric acid type A receptor subunit gamma1 (*Gabrg1*) mRNA from the set of 2438 genes uniquely dysregulated in the GRMR$^{Emx1-\text{cre}}$ hippocampus. (**E**) RTPCR of Wolframin ER transmembrane glycoprotein (*Wfs1*), gamma-aminobutyric acid type A receptor subunit alpha5 (*Gabra5*), and prostaglandin-endoperoxide synthase 2 (*Ptgs2*) mRNA from the set of 1034 genes commonly dysregulated in the MR$^{Emx1-\text{cre}}$ and GRMR$^{Emx1-\text{cre}}$ hippocampi. RTPCR data are mean ± SEM (n = 3–7 mice per group). A one-way ANOVA followed by Tukey post-hoc analysis was performed to determine significance. **P < 0.01 for MRKO compared to MRflox and for dKO compared to dflox. ***P < 0.001 for MRKO compared to MRflox and for dKO compared to dflox.

A

GRKO (413)

Rank	Diseases and Functions	p-value	Genes
1	Organismal Injury and Abnormalities	5.14E-06-2.21E-02	361
2	Cardiovascular Disease	7.99E-06-2.21E-02	40
3	Hematological Disease	7.99E-06-2.13E-02	59
4	Cancer	1.03E-05-2.21E-02	358
5	Tissue Morphology	1.03E-05-2.21E-02	80

MRKO (1478)

Rank	Diseases and Functions	p-value	Genes
1	Behavior	9.63E-10-7.17E-03	139
2	Neurological Disease	1.16E-08-8.27E-03	401
3	Organismal Injury and Abnormalities	5.32E-08-8.67E-03	1261
4	Psychological Disorders	5.32E-08-7.95E-03	232
5	Nervous System Development and Function	6.72E-08-8.2E-03	322

dKO (3637)

Rank	Diseases and Functions	p-value	Genes
1	Nervous System Development and Function	3.95E-10-1.31E-03	770
2	Tissue Development	3.95E-10-1.31E-03	848
3	Organismal Development	3.84E-09-1.31E-03	973
4	Behavior	4.46E-09-1.06E-03	297
5	Cancer	5.72E-09-1.31E-03	2976

B

MRKO (1478)

Rank	Behavior Annotation	p-Value	Act z-score	Genes
1	Cognition	9.63E-10	-1.125	94
2	Learning	1.98E-09	-1.22	87
3	Spatial learning	5.99E-06	-1.941	36
4	Motor learning	9.77E-05	0.943	12
5	Contextual conditioning	2.34E-04	0	20

dKO (3637)

Rank	Behavior Annotation	p-Value	Act z-score	Genes
1	Cognition	4.46E-09	-0.416	180
2	Learning	7.54E-09	-0.437	166
3	Memory	1.01E-04	-0.344	96
4	Locomotion	2.74E-04	1.183	120
5	Conditioning	5.72E-04	1.291	72

C

GRKO (413)

Rank	Signaling Pathways	-log(p-value)	z-score	Genes
1	Apelin Liver Signaling Pathway	3.63	-0.447	5
2	Intrinsic Prothrombin Activation Pathway	2.84	-0.447	5
3	Role of Wnt/GSK-3β Signal. in Pathogenesis of Influenza	2.54	n/a	6
4	Glioma Signaling	2.28	-1	8
5	Hepatic Fibrosis / Hepatic Stellate Cell Activation	2.19	n/a	10

MRKO (1478)

Rank	Signaling Pathways	-log(p-value)	z-score	Genes
1	CCR5 Signaling in Macrophages	4.48	0.333	19
2	nNOS Signaling in Skeletal Muscle Cells	4.46	n/a	12
3	Breast Cancer Regulation by Stathmin1	3.7	n/a	31
4	G Beta Gamma Signaling	3.59	0.447	21
5	Opioid Signaling Pathway	3.53	0	34

dKO (3637)

Rank	Signaling Pathways	-log(p-value)	z-score	Genes
1	Role of NFAT in Cardiac Hypertrophy	5.91	0.762	71
2	Opioid Signaling Pathway	5.67	0.943	74
3	GNRH Signaling	5.15	0	55
4	Fcγ Receptor-med. Phago. in Macrophages and Monocytes	4.6	1.029	34
5	G Beta Gamma Signaling	4.5	2.214	41

Fig. 5. Gene ontology analysis of dysregulated genes in the hippocampus of GR$^{Emx1\text{-cre}}$, MR$^{Emx1\text{-cre}}$, and GRMR$^{Emx1\text{-cre}}$ mice. IPA analysis was performed on the 413, 1478, and 3637 genes dysregulated in the hippocampus of the GR$^{Emx1-\text{cre}}$, MR$^{Emx1-\text{cre}}$, and GRMR$^{Emx1-\text{cre}}$ mice, respectively. (**A**) Top diseases and biological functions most significantly associated with the dysregulated genes for each knockout mouse. (**B**) Top Behavior functions most significantly associated with the dysregulated genes for the MR$^{Emx1-\text{cre}}$ and GRMR$^{Emx1-\text{cre}}$ mice. (**C**) Top signaling pathways most significantly associated with the dysregulated genes for each knockout mouse.

GRMR$^{Emx1-\text{cre}}$ mice in the second test for memory retention indicate that loss of MR signaling, rather than aberrant GR signaling, is responsible for the enhanced freezing behavior. These results suggest that MR signaling plays a critical role in normal mice regulating the expression of genes involved in fear-motivated cue learning.

3.5. Hippocampal GR and MR signaling cooperate to prevent neurodegeneration in the dentate gyrus

The large number of genes uniquely dysregulated in the GRMR$^{Emx1-\text{cre}}$ hippocampus suggests these mice may develop phenotypes distinct from their single knockout counterparts. For insight into these phenotypes, we performed a separate gene ontology analysis on these 2438 genes (Fig. 7A). Cell Death and Survival was the highest ranked cellular function associated with this gene set. Moreover, within this category, the more specific function Cell Death of Brain Cells was found to be significantly associated with the 2438 unique genes ($p = 0.0066$). A total of 60 genes belonging to the Cell Death of Brain Cells function was altered only in the double knockout hippocampus (Fig. 7B and Supplemental Table 1). This gene enrichment result suggests that the loss of both GR and MR may lead to neuronal death in the hippocampus. Since Nissl stains performed in 3-month old GRMR$^{Emx1-\text{cre}}$ mice did not reveal any major hippocampal abnormalities (Fig. 1F), we investigated the morphology of the hippocampus in 12-month old mice.

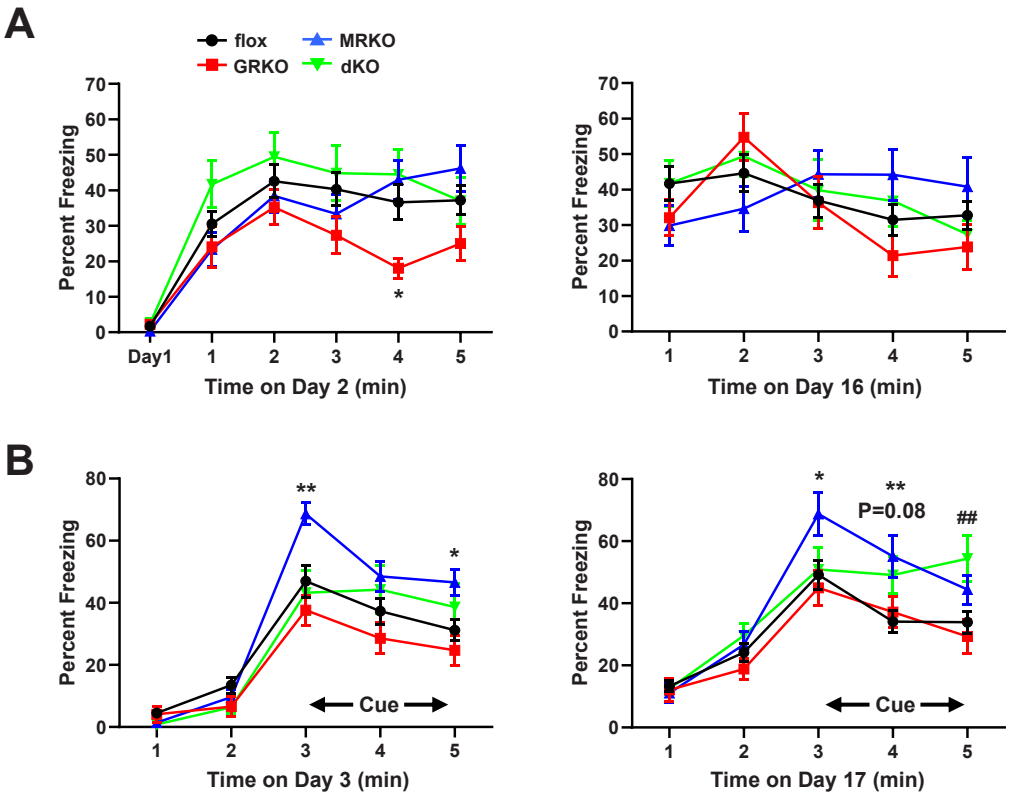

Fig. 6. MR$^{Emx1\text{-cre}}$ and GRMR$^{Emx1\text{-cre}}$ mice exhibit enhanced cue-dependent learning in a conditioned fear test. (**A**) Context-dependent learning was evaluated in male mice using the conditioned fear test. Levels of freezing were determined across a 5-min session on Day 2 (left) and Day 16 (right). (**B**) Cue-dependent learning was evaluated using the conditioned fear test. Levels of freezing were determined before and during the acoustic stimulus for the 5-min session on Day 3 (left) and Day 17 (right). Data are mean ± SEM (n = 25–27 flox mice and n = 11–12 mice per knockout group). A two-way repeated measures ANOVA followed by Tukey post-hoc analysis was performed to determine significance. *P < 0.05 for GRKO compared to flox and for MRKO compared to flox. **P < 0.01 for MRKO compared to flox. $^{\#\#}$P < 0.01 for dKO compared to flox.

Consistent with the gene ontology predictions, neurodegeneration was observed in the dentate gyrus of the GRMR$^{Emx1-cre}$ mice but not in their single knockout counterparts (Fig. 7C). The loss of granule neurons was most severe along the dorsal blade of the dentate gyrus (see arrows in Fig. 7C), resulting in a 54.4 % reduction in dorsal blade thickness (Supplemental Figure 9). Examination of the hippocampus from 4-month old double knockout mice by hematoxylin and eosin staining showed that neuronal loss was already occurring in focal regions of the dentate gyrus at this earlier time point (Fig. 7D). No neuronal loss was observed outside the hippocampus in the forebrains of the GRMR$^{Emx1-cre}$ mice. The reduction in granule neurons could reflect increased cell death and/or reduced generation of new neurons since the dentate gyrus is a critical site of adult neurogenesis (Deng et al., 2010). To assess cell death, we performed a TUNEL assay on hippocampi from younger mice at 4 months of age (Fig. 7E). A 5.4-fold increase in TUNEL-positive cells was measured in the granule cell layer of the dentate gyrus from the GRMR$^{Emx1-cre}$ mice. Neurogenesis was also evaluated in these hippocampal sections using Ki67 staining, a marker of proliferating cells, and doublecortin (DCX), a marker of neuronal precursor cells and immature neurons. We measured a 41.0 % reduction in the number of proliferating cells in the subgranular zone (SGZ) of the dentate gyrus in mice lacking both GR and MR (Fig. 7F). A 56.5 % decrease in the density of neuronal precursor cells and immature neurons was also observed in the GRMR$^{Emx1-cre}$ dentate gyrus indicating that the loss of both GR and MR results in an inhibition of neurogenesis (Fig. 7G). Consistent with this alteration in neurogenesis, Cellular Growth and Proliferation was among the top 5 cellular functions associated with the 2438 genes uniquely altered in the GRMR$^{Emx1-cre}$ hippocampus (Fig. 7A). Interestingly, the top signaling pathway associated with these genes was p53 signaling (Fig. 7A). p53 is a tumor suppressor that has been reported to regulate both proliferation during adult hippocampal neurogenesis and neuronal cell death in response to insult or injury (Miller et al., 2000; Meletis et al., 2006; Fatt et al., 2014). These data suggest that hippocampal GR and MR work together to modulate neuronal cell birth and death and preserve granule neurons of the dentate gyrus.

3.6. GR and MR associate in a complex in CA1 and dentate gyrus neurons of the hippocampus

Knockout of both GR and MR in the hippocampus resulted in the dysregulation of 2438 genes that were not altered in either of the single knockout mice. This discovery suggests that many genes rely on both GR and MR signaling pathways for their appropriate expression in the hippocampus. One point of convergence for these 2 pathways is that GR/GR and MR/MR homodimers have been reported to bind the same glucocorticoid response element (GRE) regulating target gene expression due to their highly homologous DNA binding domains (Polman et al., 2013; Mifsud and Reul, 2016). Formation of GR/MR heterodimers would provide an additional interaction point between these pathways and permit not only fine tuning of the stress response but also greater diversity in glucocorticoid signaling. To investigate whether GR and MR associate in a complex in specific neurons of the hippocampus, we performed a proximity ligation assay (PLA) on hippocampal sections from dflox control and GRMR$^{Emx1-cre}$ mice. GR/MR interaction signals were detected in CA1 pyramidal neurons and dentate gyrus granule neurons of the dflox mice but not the GRMR$^{Emx1-cre}$ mice (Fig. 8A). Quantitation of the PLA signals revealed the greatest number of GR/MR

A

dKO unique (2438)

Rank	Cellular Functions	p-value	Genes
1	Cell Death and Survival	1.82E-05-6.9E-03	709
2	Cell Morphology	2.78E-05-6.9E-03	294
3	Cellular Movement	2.78E-05-5.81E-03	407
4	Cellular Development	3.39E-05-6.9E-03	509
5	Cellular Growth and Proliferation	3.39E-05-6.9E-03	514

dKO unique (2438)

Rank	Signaling Pathways	-log(p-value)	z-score	Genes
1	p53 Signaling	4.68	-0.447	27
2	Caveolar-mediated Endocytosis Signaling	3.52	n/a	20
3	Opioid Signaling Pathway	3.23	1.021	48
4	Phospholipase C Signaling	3.22	2.197	47
5	Role of NFAT in Cardiac Hypertrophy	3.14	1.183	43

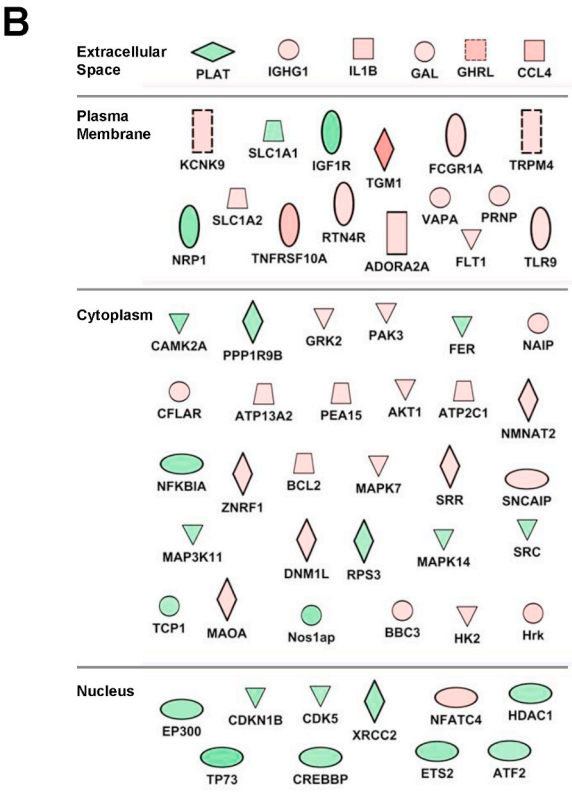

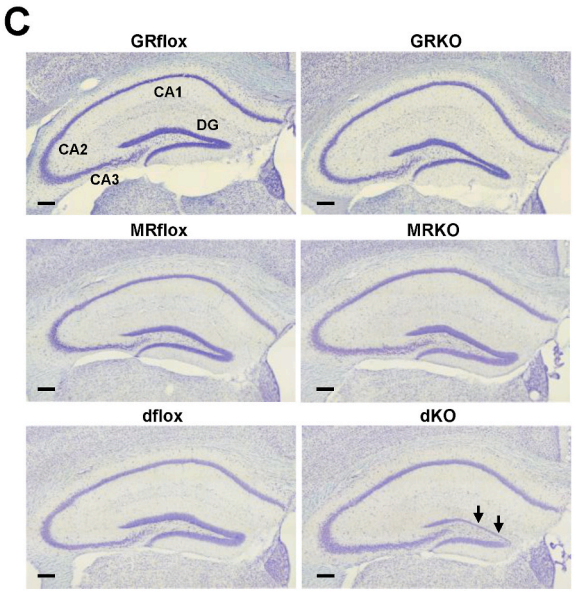

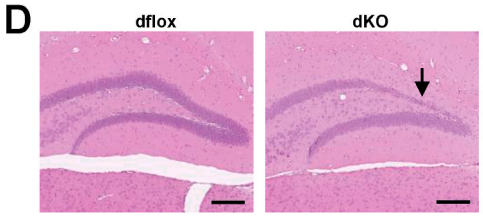

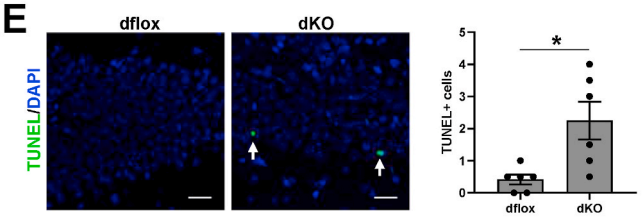

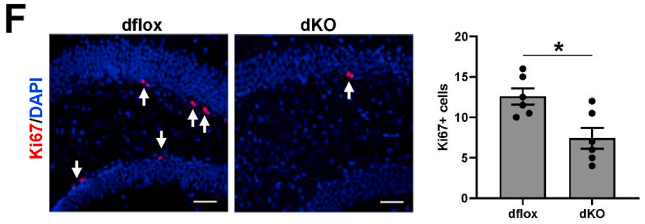

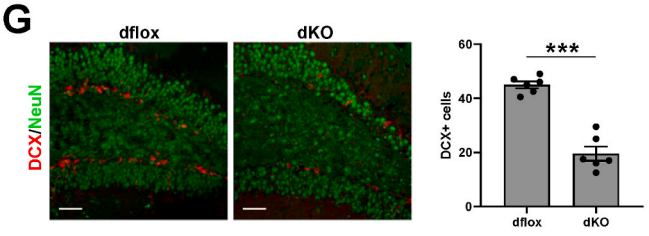

(caption on next page)

Fig. 7. GRMR$^{Emx1\text{-}cre}$ mice exhibit neurodegeneration in the dentate gyrus. (**A**) IPA analysis was performed on the 2438 genes uniquely dysregulated in the hippocampus of the GRMR$^{Emx1-cre}$ mice. Shown are the top cellular functions and signaling pathways most significantly associated with these genes. (**B**) Genes in the Cell Death of Brain Cells function that were significantly dysregulated only in the GRMR$^{Emx1-cre}$ hippocampus. Red and green colors correspond to up-regulation and down-regulation, respectively. (**C**) Representative Nissl stains of ~12-month old male mice hippocampi (n = 3–5 mice per genotype). Arrows show marked granule neuron loss along dorsal blade of dentate gyrus. Scale bars, 200 μm. (**D**) Representative hematoxylin and eosin stains of ~4-month old male mice hippocampi (n = 3 mice per genotype). Arrow shows granule neuron loss along dorsal blade of dentate gyrus. Scale bars, 200 μm. TUNEL (**E**), Ki67 (**F**), and DCX (**G**) staining of hippocampal sections from ~4-month old male mice. Shown are representative images and quantitation of TUNEL positive nuclei (arrows), Ki67-positive cells (arrows), and DCX-positive cells in the dentate gyrus. NeuN, a marker for neurons, was used in conjunction with DCX. Scale bars, 50 μm. Data are mean ± SEM (n = 6 dentate gyri per genotype). Student's *t*-test was performed to determine significance. *P < 0.05 for dKO compared to dflox. ***P < 0.001 for dKO compared to dflox.

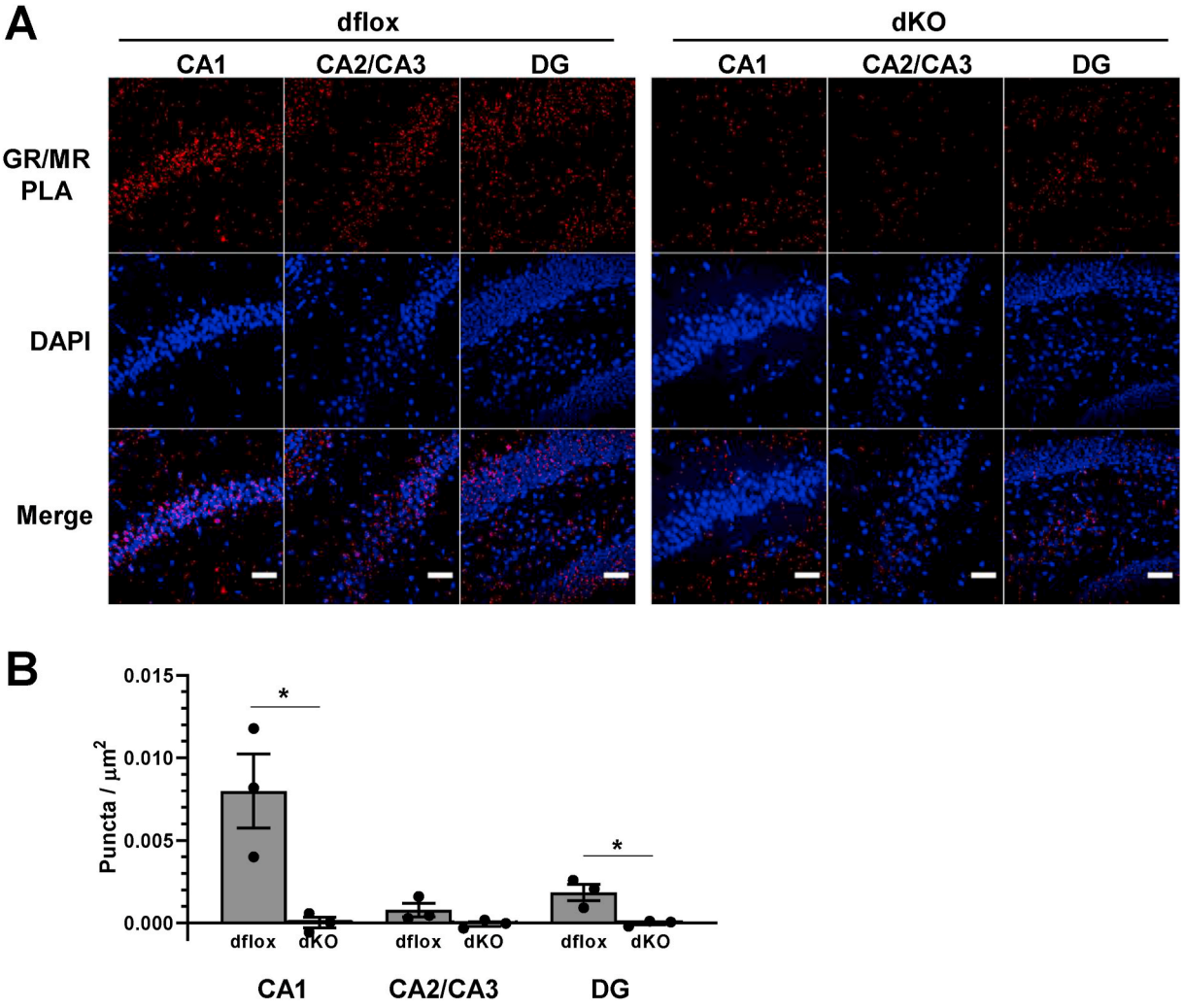

Fig. 8. GR/MR complexes in the CA1 and dentate gyrus neurons of the hippocampus. PLA was performed on hippocampal sections from male dflox control and GRMR$^{Emx1-cre}$ mice. (**A**) Representative images of the PLA GR/MR signal (red) and DAPI (blue) from the CA1, CA2/CA3, and dentate gyrus regions of the hippocampus (n = 3 mice per genotype). Each red dot represents the detection of a GR/MR complex. Scale bars, 50 μm. (**B**) Quantitation of the PLA GR/MR signal (puncta/micron^2) in the CA1, CA2/CA3, and dentate gyrus regions of the hippocampus. Data are mean ± SEM (n = 3 mice per group). Student's *t*-test was performed to determine significance. *P < 0.05 for dKO compared to dflox.

complexes in the CA1 pyramidal neurons and a smaller amount in dentate gyrus neurons of the dflox hippocampus (Fig. 8B). We detected no significant increase in PLA signals in the CA2/CA3 neurons which likely reflects their low expression of GR (Figs. 2–3). These findings demonstrate that GR and MR associate in a complex in specific hippocampal neurons and suggest that GR/MR heterodimers contribute to the combinatorial actions of stress hormone signaling in the hippocampus.

4. Discussion

We developed mice with conditional knockout of both GR and MR in the hippocampus and compared them to their single knockout counterparts in order to define individual and combinatorial actions of hippocampal GR and MR. We report that MR signaling is required for maintaining the molecular phenotype of CA2 neurons and plays an important role in cue-dependent learning. In contrast, we discovered that GR and MR work together to protect the dentate gyrus from extensive neurodegeneration by maintaining adult neurogenesis and promoting the survival of granule neurons. Ablation of both GR and MR in the hippocampus resulted in a striking expansion in the number of dysregulated genes compared to the hippocampus lacking one or the other receptor. The large cohort of genes reliant on both hippocampal GR and MR for appropriate expression was strongly associated with cell death and cell proliferation pathways. We further show that GR and MR

associate in a complex in CA1 and dentate gyrus neurons suggesting that GR/MR heterodimers contribute to the crosstalk between these two glucocorticoid signaling pathways. These data demonstrate that combinatorial actions of GR and MR are essential for maintaining the normal structure and function of the hippocampus.

CA2 neurons exhibit unique morphological, physiological, and molecular properties that distinguish them from neighboring CA1 and CA3 cells. They lack most forms of synaptic plasticity, are highly resistant to cell death, and have been implicated in a variety of diseases including autism spectrum disorder and schizophrenia (Evans et al., 2015; Dudek et al., 2016; Robert et al., 2018). The distinctive properties of CA2 neurons are conferred by selective expression of a repertoire of genes that include *Pcp4* and *Rgs14* (Evans et al., 2015; Dudek et al., 2016; McCann et al., 2021). We show that PCP4 and RGS14 expression is abolished in both the $MR^{Emx1-cre}$ and $GRMR^{Emx1-cre}$ CA2 neurons. Moreover, our genome-wide microarray data revealed altered expression of many other known CA2-specific markers in both the $MR^{Emx1-cre}$ and $GRMR^{Emx1-cre}$ mice including a reduction in adenosine A1 receptor (*Adora1*), adhesion molecule with Ig like domain 2 (*Amigo2*), N-terminal EF-hand calcium binding protein 2 (*Necab2*), calbindin 1 (*Calb1*), SPARC related modular calcium binding 2 (*Smoc2*), and striatin interacting protein 2 (*Strip2*) mRNA and an increase in formin homology 2 domain containing 3 (*Fhod3*) mRNA. Our finding that multiple CA2-specific markers are altered in a similar manner in both the $MR^{Emx1-cre}$ and $GRMR^{Emx1-cre}$ hippocampi indicates that a deficiency in MR signaling, rather than aberrant GR signaling, underlies these gene changes. This is an important distinction given the marked increase in GR expression that occurs in CA2 neurons depleted of MR. Thus, our data demonstrate that MR signaling plays a critical role regulating the molecular profile of CA2 neurons. Mice with conditional knockout of MR in the hippocampus have been reported previously to show alterations in the expression of CA2 neuronal markers (McCann et al., 2021); however whether the loss of MR signaling or aberrant GR signaling accounted for these gene changes was not considered.

Our global transcriptional analysis demonstrated that many genes were commonly dysregulated in the $MR^{Emx1-cre}$ and $GRMR^{Emx1-cre}$ hippocampi. The gene changes were strongly associated with behavior and, more specifically, cognition. Consistent with this gene enrichment result, both of these mouse models displayed enhanced cue-dependent learning in a conditioned fear test which suggests the loss of MR signaling, rather than aberrant GR signaling, underlies this behavioral change. These findings are in accord with previous studies reporting alterations in fear motivated cue memory in mice with conditional knockout of MR in the forebrain (Ter Horst et al., 2012). How MR signaling regulates fear memory remains poorly understood. Our gene ontology analysis suggests changes in GPCR signaling pathways may be prominently involved. GPCRs are abundant in the hippocampus, play important roles in its cognitive and affective functions, and have been implicated in the etiology of many psychiatric disorders (Catapano and Manji, 2007). These receptors alter synaptic transmission through pre-synaptic and post-synaptic regulation of neurotransmitter release and are involved in both long-term potentiation and long-term depression. Findings from the $MR^{Emx1-cre}$ and $GRMR^{Emx1-cre}$ mice suggest that opioid and G beta gamma signaling pathways might be especially sensitive to regulation by MR signaling. Interestingly, CA2 neurons have been reported to constrain learning and memory by limiting synaptic plasticity, and this effect appears to be dependent on their expression of RGS14 and the adenosine A1 receptor (Lee et al., 2010; Simons et al., 2011). RGS14 regulates GPCR intracellular signaling cascades and the adenosine A1 receptor is a GPCR, and both these genes are reduced in $MR^{Emx1-cre}$ and $GRMR^{Emx1-cre}$ hippocampi. The reduced expression of these two genes in CA2 neurons and the consequent acquisition of long-term potentiation may contribute to the stronger fear memory observed in these knockout mice.

For further insight into the mechanisms responsible for the altered fear memories in the $MR^{Emx1-cre}$ and $GRMR^{Emx1-cre}$ mice, it will be important to complement our transcriptomic analysis of the hippocampus with a proteomics approach to capture the global protein changes following the loss of GR, MR, or both GR and MR in the hippocampus. In addition, given the known roles of glucocorticoids to regulate neuronal cytoarchitecture and hippocampus network connectivity (McEwen et al., 2016; Cameron and Schoenfeld, 2018), it will be critical to evaluate synaptic plasticity in the single and double knockout mice. In this regard, we have recently demonstrated that the $GR^{Emx1-cre}$ mice exhibit reductions in CA1 neuronal arborization and dendritic spine density, suggesting these mice may have deficits in learning and memory (Tejos-Bravo et al., 2021). Furthermore, it will be important to examine HPA axis regulation in our single and double knockout mice when exposed to different stress paradigms since abnormalities in HPA activity can impact behavior. While we did not detect alterations in the circadian levels of corticosterone nor in the peak levels of corticosterone induced by acute restraint stress, it is possible that the knockout mice differ in their kinetics of HPA axis activation and/or in the negative feedback profile of HPA axis inhibition. It should be noted that several studies have shown that conditional knockout of GR in the forebrain can lead to dysregulation of the HPA axis (Boyle et al., 2005, 2006; Furay et al., 2008; Solomon et al., 2012). Other studies, however, have reported that HPA axis activity is unaltered following GR depletion in the forebrain which is consistent with our own current findings (Vincent et al., 2013). The reason for these conflicting results is unclear but likely involves differences in testing regimens, the pattern of GR deletion in the forebrain, and/or the genetic background of the mice. Finally, a limitation to defining the mechanisms underlying the altered fear memory in our single and double knockout mice is that receptor loss is not restricted to the hippocampus but occurs in several other regions of the forebrain such as the cortex and parts of the amygdala. Depletion of GR and MR in these extra hippocampal regions may also contribute to observed behavioral phenotypes.

An unexpected finding from our transcriptomic analysis of the knockout mice was the large increase in dysregulated genes that occurred only in the hippocampus depleted of both GR and MR. This result suggests that many genes depend on both GR and MR signaling for their appropriate expression in the hippocampus. This set of unique genes was strongly associated with cell death and cell proliferation pathways. In agreement with the gene enrichment analysis, the $GRMR^{Emx1-cre}$ mice, but not their single knockout counterparts, exhibited extensive neurodegeneration in the dentate gyrus. The loss of granule neurons was evident by 4 months of age and even more pronounced in older $GRMR^{Emx1-cre}$ mice. Both an increase in neuronal death and a reduction in neurogenesis appear to contribute to the neuronal loss in the hippocampus depleted of both GR and MR. Glucocorticoids have been shown to promote the survival of granule neurons as the removal of endogenous glucocorticoids by adrenalectomy results in their death (Schoenfeld and Gould, 2013). This protective effect has been attributed to MR based on replacement experiments with receptor-selective agonists and by the occurrence of granule neuron death in whole body MR null mice (Gass et al., 2000; Schoenfeld and Gould, 2013). On the other hand, activation of GR by the synthetic agonist dexamethasone has been reported to stimulate apoptosis of neurons in the dentate gyrus suggesting GR and MR may have opposing actions on neuronal death (Hassan et al., 1996). These studies, however, do not discriminate between hippocampal and systemic glucocorticoid signaling. Our single knockout mice lacking MR alone or GR alone in the hippocampus did not exhibit neurodegeneration which is in accord with other mouse models with genetic deletion of one or the other receptor in the forebrain (Tronche et al., 1999; Gass et al., 2000; Berger et al., 2006). Only when both hippocampal GR and MR were depleted was neuronal loss observed indicating that both receptors work together in normal mice to promote the survival of granule neurons. While findings from our TUNEL assay suggest that granule neurons exhibit increased cell death in the dentate gyrus of the double knockout mice, it is also possible that the survival of neural progenitors in the neurogenic niche

has been compromised and contributes to the phenotype. Glucocorticoids have been shown to regulate the life span of these cells. Interestingly, the systemic loss of glucocorticoid signaling by adrenalectomy promotes the survival of newly-formed progenitors in the dentate gyrus (Wong and Herbert, 2004).

In addition to regulating neuronal death, glucocorticoids also have a major impact on adult hippocampal neurogenesis (Schoenfeld and Gould, 2013; Egeland et al., 2015). This process contributes to the structural and functional plasticity of the hippocampus and plays a critical role in memory formation and mood regulation. Multiple studies using pharmacological agents to manipulate receptor activity have reported that glucocorticoids inhibit adult neurogenesis via GR signaling (Egeland et al., 2015). The role played by MR signaling is less clear as both stimulatory and inhibitory effects on cell proliferation and neurogenesis have been described (Wong and Herbert, 2005). The reduction in immature neurons observed in our double knockout mice indicate that both hippocampal GR and MR signaling are important for maintaining appropriate levels of adult neurogenesis in the dentate gyrus. Since adult neural stem cells can also give rise to astrocytes, an important consideration for future studies will be to investigate whether gliogenesis is also altered in the dentate gyrus of $GRMR^{Emx1-cre}$ mice. Gene enrichment analysis identified p53 signaling as the top pathway associated with the large set of 2438 genes uniquely altered in the $GRMR^{Emx1-cre}$ hippocampus. p53 is a tumor suppressor that plays an important role in both neuronal cell death and adult hippocampal neurogenesis (Meletis et al., 2006; Fatt et al., 2014). Glucocorticoids operating through GR have been reported to inhibit p53-dependent transcriptional activity, cell cycle arrest, and apoptosis in human neuroblastoma cells via sequestration of p53 in the cytoplasm (Sengupta et al., 2000). In addition, MR signaling has been suggested to down-regulate p53 expression in the hippocampus of rats (McCullers and Herman, 1998; Almeida et al., 2000). Therefore, an increase in p53 activity due to the deficiency of both GR and MR might account for both the increased granule neuron death and the reduced neurogenesis in $GRMR^{Emx1-cre}$ dentate gyrus. The functional interplay between hippocampal GR and MR in both cell death and cell proliferation processes highlights the critical nature of granule neurons for behavioral adaptations to stress.

The synergistic increase in the number of dysregulated genes following the loss of both GR and MR in the hippocampus suggests that combinatorial actions of these two receptors comprise a critical component of the stress response. GR and MR have been postulated to heterodimerize based on in vitro studies using over-expressed proteins (Trapp et al., 1994; Liu et al., 1995; Savory et al., 2001; Nishi et al., 2004). Formation of GR/MR heterodimers has also been suggested by recent work reporting that GR and MR are recruited to the same GRE-containing DNA fragment in rat hippocampal lysates (Mifsud and Reul, 2016). GR/MR interactions would allow crosstalk to occur between GR and MR glucocorticoid signaling pathways. Using the PLA assay, we now demonstrate in situ that GR and MR associate in a complex in CA1 pyramidal neurons and dentate gyrus granule neurons. Since GR/MR interactions can confer unique transcriptional responses to glucocorticoids on target genes (Rivers et al., 2019), the presence of GR/GR homodimers, MR/MR homodimers, and GR/MR heterodimers in the hippocampus would allow for more intricate regulation of glucocorticoid-responsive genes and provide a mechanism for greater diversity in stress hormone action.

5. Conclusion

In conclusion, we developed mice for the first time with conditional knockout of both GR and MR in the hippocampus and compared them to their single knockout counterparts. We discovered that MR signaling is required for maintaining the molecular phenotype of CA2 neurons. In contrast, GR and MR work together to protect the dentate gyrus from neurodegeneration by maintaining adult neurogenesis and promoting the survival of granule neurons. These findings will inform new strategies for treating stress-related learning and memory deficits and psychiatric illnesses.

CRediT authorship contribution statement

Robert H. Oakley: Conceptualization, Methodology, Investigation, Writing – original draft, Writing – review & editing. **Shannon D. Whirledge:** Conceptualization, Methodology, Investigation, Writing – review & editing. **Maria G. Petrillo:** Methodology, Investigation, Writing – review & editing. **Natallia V. Riddick:** Methodology, Investigation. **Xiaojiang Xu:** Methodology, Formal analysis, Investigation, Writing – review & editing. **Sheryl S. Moy:** Methodology, Investigation, Writing – original draft, Writing – review & editing, Supervision, Funding acquisition. **John A. Cidlowski:** Conceptualization, Methodology, Writing – original draft, Writing – review & editing, Supervision, Funding acquisition.

Declaration of competing interest

The authors declare that they have no known competing financial interests or personal relationships that could have appeared to influence the work reported in this paper.

Acknowledgements

We thank Dr. Pierre Chambon (Institut de Génétique et de Biologie Moléculaire et Cellulaire) for provision of the MR-flox mice, Dr. Kevin Gerrish of the Molecular Genomics Core Facility (NIEHS) for assistance with microarray analyses, Charles J. Tucker and Erica Scappini of the Fluorescence Microscopy and Imaging Center (NIEHS) for assistance with confocal microscopy and PLA quantitation, Steven E. Butler of the Comparative Medicine Branch (NIEHS) for assistance with blood collection from mice, and Dr. Matthew Quinn of the Signal Transduction Laboratory (NIEHS) for assistance with tissue isolation. This research was supported by the Intramural Research Program of the NIH, NIEHS (1ZIAES090057-24). The UNC Mouse Behavioral Phenotyping Core is supported by NICHD; U54 HD079124.

Appendix A. Supplementary data

Supplementary data to this article can be found online at https://doi.org/10.1016/j.ynstr.2021.100369.

Data statement

The authors declare that all supporting data are available within the article, or from the corresponding author, upon reasonable request.

References

Almeida, O.F., Conde, G.L., Crochemore, C., Demeneix, B.A., Fischer, D., Hassan, A.H., Meyer, M., Holsboer, F., Michaelidis, T.M., 2000. Subtle shifts in the ratio between pro- and antiapoptotic molecules after activation of corticosteroid receptors decide neuronal fate. Faseb. J. 14, 779–790.

Berger, S., Bleich, M., Schmid, W., Cole, T.J., Peters, J., Watanabe, H., Kriz, W., Warth, R., Greger, R., Schutz, G., 1998. Mineralocorticoid receptor knockout mice: pathophysiology of Na+ metabolism. Proc. Natl. Acad. Sci. U. S. A. 95, 9424–9429.

Berger, S., Wolfer, D.P., Selbach, O., Alter, H., Erdmann, G., Reichardt, H.M., Chepkova, A.N., Welzl, H., Haas, H.L., Lipp, H.P., Schutz, G., 2006. Loss of the limbic mineralocorticoid receptor impairs behavioral plasticity. Proc. Natl. Acad. Sci. U. S. A. 103, 195–200.

Boyle, M.P., Brewer, J.A., Funatsu, M., Wozniak, D.F., Tsien, J.Z., Izumi, Y., Muglia, L.J., 2005. Acquired deficit of forebrain glucocorticoid receptor produces depression-like changes in adrenal axis regulation and behavior. Proc. Natl. Acad. Sci. U. S. A. 102, 473–478.

Boyle, M.P., Kolber, B.J., Vogt, S.K., Wozniak, D.F., Muglia, L.J., 2006. Forebrain glucocorticoid receptors modulate anxiety-associated locomotor activation and adrenal responsiveness. J. Neurosci. 26, 1971–1978.

Cameron, H.A., Schoenfeld, T.J., 2018. Behavioral and structural adaptations to stress. Front. Neuroendocrinol. 49, 106–113.
Catapano, L.A., Manji, H.K., 2007. G protein-coupled receptors in major psychiatric disorders. Biochim. Biophys. Acta 1768, 976–993.
de Kloet, E.R., Joels, M., Holsboer, F., 2005. Stress and the brain: from adaptation to disease. Nat. Rev. Neurosci. 6, 463–475.
De Kloet, E.R., Vreugdenhil, E., Oitzl, M.S., Joels, M., 1998. Brain corticosteroid receptor balance in health and disease. Endocr. Rev. 19, 269–301.
Deng, W., Aimone, J.B., Gage, F.H., 2010. New neurons and new memories: how does adult hippocampal neurogenesis affect learning and memory? Nat. Rev. Neurosci. 11, 339–350.
Dudek, S.M., Alexander, G.M., Farris, S., 2016. Rediscovering area CA2: unique properties and functions. Nat. Rev. Neurosci. 17, 89–102.
Egeland, M., Zunszain, P.A., Pariante, C.M., 2015. Molecular mechanisms in the regulation of adult neurogenesis during stress. Nat. Rev. Neurosci. 16, 189–200.
Evans, P.R., Dudek, S.M., Hepler, J.R., 2015. Regulator of G Protein signaling 14: a molecular brake on synaptic plasticity linked to learning and memory. Prog Mol Biol Transl Sci 133, 169–206.
Fatt, M.P., Cancino, G.I., Miller, F.D., Kaplan, D.R., 2014. p63 and p73 coordinate p53 function to determine the balance between survival, cell death, and senescence in adult neural precursor cells. Cell Death Differ. 21, 1546–1559.
Furay, A.R., Bruestle, A.E., Herman, J.P., 2008. The role of the forebrain glucocorticoid receptor in acute and chronic stress. Endocrinology 149, 5482–5490.
Gass, P., Kretz, O., Wolfer, D.P., Berger, S., Tronche, F., Reichardt, H.M., Kellendonk, C., Lipp, H.P., Schmid, W., Schutz, G., 2000. Genetic disruption of mineralocorticoid receptor leads to impaired neurogenesis and granule cell degeneration in the hippocampus of adult mice. EMBO Rep. 1, 447–451.
Gomez-Sanchez, C.E., de Rodriguez, A.F., Romero, D.G., Estess, J., Warden, M.P., Gomez-Sanchez, M.T., Gomez-Sanchez, E.P., 2006. Development of a panel of monoclonal antibodies against the mineralocorticoid receptor. Endocrinology 147, 1343–1348.
Gorski, J.A., Talley, T., Qiu, M., Puelles, L., Rubenstein, J.L., Jones, K.R., 2002. Cortical excitatory neurons and glia, but not GABAergic neurons, are produced in the Emx1-expressing lineage. J. Neurosci. 22, 6309–6314.
Hassan, A.H., von Rosenstiel, P., Patchev, V.K., Holsboer, F., Almeida, O.F., 1996. Exacerbation of apoptosis in the dentate gyrus of the aged rat by dexamethasone and the protective role of corticosterone. Exp. Neurol. 140, 43–52.
Lee, S.E., Simons, S.B., Heldt, S.A., Zhao, M., Schroeder, J.P., Vellano, C.P., Cowan, D.P., Ramineni, S., Yates, C.K., Feng, Y., Smith, Y., Sweatt, J.D., Weinshenker, D., Ressler, K.J., Dudek, S.M., Hepler, J.R., 2010. RGS14 is a natural suppressor of both synaptic plasticity in CA2 neurons and hippocampal-based learning and memory. Proc. Natl. Acad. Sci. U. S. A. 107, 16994–16998.
Liu, W., Wang, J., Sauter, N.K., Pearce, D., 1995. Steroid receptor heterodimerization demonstrated in vitro and in vivo. Proc. Natl. Acad. Sci. U. S. A. 92, 12480–12484.
McCann, K.E., Lustberg, D.J., Shaughnessy, E.K., Carstens, K.E., Farris, S., Alexander, G. M., Radzicki, D., Zhao, M., Dudek, S.M., 2021. Novel role for mineralocorticoid receptors in control of a neuronal phenotype. Mol. Psychiatr. 26, 350–364.
McCullers, D.L., Herman, J.P., 1998. Mineralocorticoid receptors regulate bcl-2 and p53 mRNA expression in hippocampus. Neuroreport 9, 3085–3089.
McCurley, A., Pires, P.W., Bender, S.B., Aronovitz, M., Zhao, M.J., Metzger, D., Chambon, P., Hill, M.A., Dorrance, A.M., Mendelsohn, M.E., Jaffe, I.Z., 2012. Direct regulation of blood pressure by smooth muscle cell mineralocorticoid receptors. Nat. Med. 18, 1429–1433.
McEwen, B.S., Nasca, C., Gray, J.D., 2016. Stress Effects on Neuronal Structure: Hippocampus, Amygdala, and Prefrontal Cortex. Neuropsychopharmacology, vol. 41. official publication of the American College of Neuropsychopharmacology, pp. 3–23.
Meletis, K., Wirta, V., Hede, S.M., Nister, M., Lundeberg, J., Frisen, J., 2006. p53 suppresses the self-renewal of adult neural stem cells. Development 133, 363–369.
Mifsud, K.R., Reul, J.M., 2016. Acute stress enhances heterodimerization and binding of corticosteroid receptors at glucocorticoid target genes in the hippocampus. Proc. Natl. Acad. Sci. U. S. A. 113, 11336–11341.
Miller, F.D., Pozniak, C.D., Walsh, G.S., 2000. Neuronal life and death: an essential role for the p53 family. Cell Death Differ. 7, 880–888.
Nishi, M., Tanaka, M., Matsuda, K., Sunaguchi, M., Kawata, M., 2004. Visualization of glucocorticoid receptor and mineralocorticoid receptor interactions in living cells with GFP-based fluorescence resonance energy transfer. J. Neurosci. 24, 4918–4927.
Oakley, R.H., Cidlowski, J.A., 2013. The biology of the glucocorticoid receptor: new signaling mechanisms in health and disease. J. Allergy Clin. Immunol. 132, 1033–1044.
Oakley, R.H., Cruz-Topete, D., He, B., Foley, J.F., Myers, P.H., Xu, X., Gomez-Sanchez, C. E., Chambon, P., Willis, M.S., Cidlowski, J.A., 2019. Cardiomyocyte glucocorticoid and mineralocorticoid receptors directly and antagonistically regulate heart disease in mice. Sci. Signal. 12.
Oakley, R.H., Ren, R., Cruz-Topete, D., Bird, G.S., Myers, P.H., Boyle, M.C., Schneider, M. D., Willis, M.S., Cidlowski, J.A., 2013. Essential role of stress hormone signaling in cardiomyocytes for the prevention of heart disease. Proc. Natl. Acad. Sci. U. S. A. 110, 17035–17040.
Polman, J.A., de Kloet, E.R., Datson, N.A., 2013. Two populations of glucocorticoid receptor-binding sites in the male rat hippocampal genome. Endocrinology 154, 1832–1844.
Reul, J.M., de Kloet, E.R., 1985. Two receptor systems for corticosterone in rat brain: microdistribution and differential occupation. Endocrinology 117, 2505–2511.
Rivers, C.A., Rogers, M.F., Stubbs, F.E., Conway-Campbell, B.L., Lightman, S.L., Pooley, J.R., 2019. Glucocorticoid receptor-tethered mineralocorticoid receptors increase glucocorticoid-induced transcriptional responses. Endocrinology 160, 1044–1056.
Robert, V., Cassim, S., Chevaleyre, V., Piskorowski, R.A., 2018. Hippocampal area CA2: properties and contribution to hippocampal function. Cell Tissue Res. 373, 525–540.
Savory, J.G., Prefontaine, G.G., Lamprecht, C., Liao, M., Walther, R.F., Lefebvre, Y.A., Hache, R.J., 2001. Glucocorticoid receptor homodimers and glucocorticoid-mineralocorticoid receptor heterodimers form in the cytoplasm through alternative dimerization interfaces. Mol. Cell Biol. 21, 781–793.
Schoenfeld, T.J., Gould, E., 2013. Differential effects of stress and glucocorticoids on adult neurogenesis. Curr Top Behav Neurosci 15, 139–164.
Seckl, J.R., Dickson, K.L., Yates, C., Fink, G., 1991. Distribution of glucocorticoid and mineralocorticoid receptor messenger RNA expression in human postmortem hippocampus. Brain Res. 561, 332–337.
Sengupta, S., Vonesch, J.L., Waltzinger, C., Zheng, H., Wasylyk, B., 2000. Negative cross-talk between p53 and the glucocorticoid receptor and its role in neuroblastoma cells. EMBO J. 19, 6051–6064.
Simons, S.B., Caruana, D.A., Zhao, M., Dudek, S.M., 2011. Caffeine-induced synaptic potentiation in hippocampal CA2 neurons. Nat. Neurosci. 15, 23–25.
Solomon, M.B., Furay, A.R., Jones, K., Packard, A.E., Packard, B.A., Wulsin, A.C., Herman, J.P., 2012. Deletion of forebrain glucocorticoid receptors impairs neuroendocrine stress responses and induces depression-like behavior in males but not females. Neuroscience 203, 135–143.
Tejos-Bravo, M., Oakley, R.H., Whirledge, S.D., Corrales, W.A., Silva, J.P., Garcia-Rojo, G., Toledo, J., Sanchez, W., Roman-Albasini, L., Aliaga, E., Aguayo, F., Olave, F., Maracaja-Coutinho, V., Cidlowski, J.A., Fiedler, J.L., 2021. Deletion of hippocampal Glucocorticoid receptors unveils sex-biased microRNA expression and neuronal morphology alterations in mice. Neurobiol Stress 14, 100306.
Ter Horst, J.P., Carobrez, A.P., van der Mark, M.H., de Kloet, E.R., Oitzl, M.S., 2012. Sex differences in fear memory and extinction of mice with forebrain-specific disruption of the mineralocorticoid receptor. Eur. J. Neurosci. 36, 3096–3102.
ter Horst, J.P., van der Mark, M.H., Arp, M., Berger, S., de Kloet, E.R., Oitzl, M.S., 2012. Stress or no stress: mineralocorticoid receptors in the forebrain regulate behavioral adaptation. Neurobiol. Learn. Mem. 98, 33–40.
Trapp, T., Rupprecht, R., Castren, M., Reul, J.M., Holsboer, F., 1994. Heterodimerization between mineralocorticoid and glucocorticoid receptor: a new principle of glucocorticoid action in the CNS. Neuron 13, 1457–1462.
Tronche, F., Kellendonk, C., Kretz, O., Gass, P., Anlag, K., Orban, P.C., Bock, R., Klein, R., Schutz, G., 1999. Disruption of the glucocorticoid receptor gene in the nervous system results in reduced anxiety. Nat. Genet. 23, 99–103.
Vincent, M.Y., Hussain, R.J., Zampi, M.E., Sheeran, K., Solomon, M.B., Herman, J.P., Khan, A., Jacobson, L., 2013. Sensitivity of depression-like behavior to glucocorticoids and antidepressants is independent of forebrain glucocorticoid receptors. Brain Res. 1525, 1–15.
Watzka, M., Beyenburg, S., Blumcke, I., Elger, C.E., Bidlingmaier, F., Stoffel-Wagner, B., 2000. Expression of mineralocorticoid and glucocorticoid receptor mRNA in the human hippocampus. Neurosci. Lett. 290, 121–124.
Wong, E.Y., Herbert, J., 2004. The corticoid environment: a determining factor for neural progenitors' survival in the adult hippocampus. Eur. J. Neurosci. 20, 2491–2498.
Wong, E.Y., Herbert, J., 2005. Roles of mineralocorticoid and glucocorticoid receptors in the regulation of progenitor proliferation in the adult hippocampus. Eur. J. Neurosci. 22, 785–792.
Xie, X., Yang, H., An, J.J., Houtz, J., Tan, J.W., Xu, H., Liao, G.Y., Xu, Z.X., Xu, B., 2019. Activation of anxiogenic circuits instigates resistance to diet-induced obesity via increased energy expenditure. Cell Metabol. 29, 917–931 e914.